

On Erlang mixture approximations for differential equations with distributed time delays

Tobias K. S. Ritschel*

Abstract. In this paper, we propose a general approach for approximate simulation and analysis of delay differential equations (DDEs) with distributed time delays based on methods for ordinary differential equations (ODEs). The key innovation is that we 1) approximate the kernel by the probability density function of an Erlang mixture and 2) use the linear chain trick to transform the approximate DDEs to ODEs. Furthermore, we prove that an approximation with infinitely many terms converges for continuous and bounded kernels and for specific choices of the coefficients. We compare the steady states of the original DDEs and their stability criteria to those of the approximate system of ODEs, and we propose an approach based on bisection and least-squares estimation for determining optimal parameter values in the approximation. Finally, we present numerical examples that demonstrate the accuracy and convergence rate obtained with the optimal parameters and the efficacy of the proposed approach for bifurcation analysis and Monte Carlo simulation. The numerical examples involve a modified logistic equation and a point reactor kinetics model of a molten salt nuclear fission reactor.

Key words. Mixture approximations, distributed time delays, delay differential equations, linear chain trick.

MSC codes. 37M05, 39B99, 41A30, 65D15, 65P99, 65Q20

1. Introduction. Many industrial and natural processes exhibit time delays [28], e.g., due to advection (flow in a pipe or river), diffusion (mixing), or feedback mechanisms (natural or man-made), and as time delays can have a significant impact on the dynamics and stability of a process [36], it is important to account for them when developing and analyzing mathematical models. Such models typically involve differential equations, and the time delays can either be absolute (discrete) or distributed (continuous) [47]. In the former case, the right-hand side function depends on the state at specific points in the past, and in the latter, it depends on a weighted integral of all past states, i.e., a convolution. The weight function is called the kernel or memory function. Although discrete time delays are more commonly used, they typically arise from a simplification of the underlying phenomena. For instance, assuming plug-flow in a pipe leads to an absolute time delay whereas a nonuniform flow velocity (e.g., Hagen-Poiseuille flow) leads to a distributed delay [41]. In this work, we focus on the latter.

In recent decades, there has been a significant interest in distributed time delays, and they have been used to model a variety of processes, e.g., in pharmacokinetics and pharmacodynamics (PK/PD) [21], neuroscience [1], side-effects of chemotherapy [31], the Mackey-Glass system [35, 56], which can describe respiratory and hematopoietic diseases, population models in biology [9], and pollution in fisheries [6]. Mechanical [2] and economic [17] processes have also been considered, and we refer to the book by Kolmanovskii and Myshkis [28] for more examples. Furthermore, many theoretical results have been developed specifically for DDEs with distributed time delays. Rahman et al. [40] studied the stability of networked systems

*Department of Applied Mathematics and Computer Science, Technical University of Denmark, DK-2800 Kgs. Lyngby, Denmark (tobk@dtu.dk).

with distributed delays, Yuan and Belair [54] present general stability and bifurcation results, Bazighifan et al. [4] analyze oscillations in higher-order DDEs with distributed delays, Cassidy [8] demonstrate the equivalence between cyclic ordinary differential equations (ODEs) and a scalar DDE with a distributed delay, and Aleksandrov et al. [3] study the stability of systems with state-dependent kernels.

Despite the many applications, there exists far less theory and fewer numerical methods and software for DDEs with distributed time delays than for ODEs. Even for DDEs with absolute delays, there exist many numerical methods [5, 37] and significant amounts of off-the-shelf software, e.g., for simulation [46]. However, some modeling software does contain functionality for distributed time delays, e.g., NONMEM [53] and Phoenix [21], and customized numerical methods have also been proposed. Typically, they 1) approximate the integral in the convolution using a quadrature rule, e.g., a trapezoidal [22] or Gaussian [50] rule, and 2) discretize the differential equations using a one-step method, e.g., a Runge-Kutta method [56, 16], or a linear multistep method [51]. Methods based on splines have also been proposed [57]. However, compared to similar methods for ODEs, approximating the convolution is requiring in terms of computations and memory, and it is not straightforward to choose the time step size adaptively.

Consequently, it is desirable to identify approaches that can directly take advantage of existing theory, methods, and software for ODEs, and for a specific class of kernels, it is possible to transform DDEs with distributed delays to ODEs. Specifically, the transformation is called the *linear chain trick* (LCT) [33, 38, 47], and it is applicable when the kernel is given by the probability density function of an Erlang distribution (referred to as an Erlang kernel). The LCT has been widely used, and Hurtado and Kiro Singh [23] and Hurtado and Richards [24, 25] generalized it to transform a wider range of stochastic mean field models to ODEs. Additionally, both Cassidy et al. [10] and Krzyzanski [30] have proposed to simplify the simulation and analysis of specific DDEs by approximating the involved gamma kernels by a hypoexponential kernel and a truncated binomial series, respectively. However, to the best of the author's knowledge, there are no general-purpose LCTs or approximations for broader classes of kernels.

Therefore, in this work, we present a general-purpose Erlang mixture approximation for continuous and bounded kernels, which allows us to use the LCT to approximate a large class of DDEs with distributed time delays by ODEs. We prove that the approximation converges, and we compare the stability criteria for the approximate ODEs and the original system. Furthermore, we propose a least-squares approach for determining the Erlang mixture approximation coefficients and rate parameter, and we use a numerical example to demonstrate that such an optimal approximation is more accurate than an approximation which uses theoretical coefficients from the proof. Finally, using two numerical examples, we demonstrate that the proposed approach can be used to approximately simulate and analyze the solution of DDEs with distributed time delays.

The remainder of the paper is structured as follows. In Section 2 and 3, we present the notation used and the system considered in this paper, respectively. Next, in Section 4, we present the mixed Erlang approximation and prove that it converges, and in Section 5, we describe how to use the LCT to transform the approximate system of DDEs to a set of ODEs. In Section 6, we describe the least-squares approach, and in Section 7 and 8, we present

numerical examples. Finally, conclusions are presented in Section 9.

2. Preliminaries. The spaces $\mathbb{R}_{\geq 0} = \{x \in \mathbb{R} | x \geq 0\}$ and $\mathbb{N}_{\geq 0} = \{0, 1, \dots\}$ contain the non-negative real numbers and integers, respectively, and $\mathbb{R}_{> 0} = \{x \in \mathbb{R} | x > 0\}$ is the space of positive real numbers. We denote by \odot the Hadamard (or elementwise) product (also called the Schur product) [19, 20], i.e., if $c = a \odot b$, then $c_i = a_i b_i$. Furthermore, $\det A$ is the determinant of the matrix argument, A , and $\text{diag } a$ denotes a diagonal matrix whose diagonal elements are the elements of the vector (or set) argument, a , i.e., if $C = \text{diag } a$, then $C_{ii} = a_i$ and $C_{ij} = 0$ for $i \neq j$. We will make repeated use of the identity

$$(2.1) \quad e^{at} = \sum_{m=0}^{\infty} \frac{(at)^m}{m!}$$

in the proofs in Section 4.1, and we denote by $[\cdot]^+ = \max\{0, \cdot\}$ the positive part of the argument.

3. System. We consider systems in the form

$$(3.1a) \quad x(t) = x_0(t), \quad t \in (-\infty, t_0],$$

$$(3.1b) \quad \dot{x}(t) = f(x(t), z(t)), \quad t \in [t_0, t_f],$$

where $t \in \mathbb{R}$ is time, $t_0, t_f \in \mathbb{R}$ are the initial and final time, $x : \mathbb{R} \rightarrow \mathbb{R}^{n_x}$ is the state, and $x_0 : \mathbb{R} \rightarrow \mathbb{R}^{n_x}$ is the initial state function. Furthermore, $f : \mathbb{R}^{n_x} \times \mathbb{R}^{n_z} \rightarrow \mathbb{R}^{n_x}$ is the right-hand side function, and the memory state, $z : \mathbb{R} \rightarrow \mathbb{R}^{n_z}$, is given by the convolution

$$(3.2a) \quad z(t) = \int_{-\infty}^t \alpha(t-s) \odot r(s) ds,$$

$$(3.2b) \quad r(t) = h(x(t)),$$

where $r : \mathbb{R} \rightarrow \mathbb{R}^{n_z}$ is the delayed variable, and each element of $\alpha : \mathbb{R}_{\geq 0} \rightarrow \mathbb{R}_{\geq 0}^{n_z}$ is a *regular* kernel (see Definition 3.1). Furthermore, $h : \mathbb{R}^{n_x} \rightarrow \mathbb{R}^{n_z}$ is the memory function. We assume that f and h are differentiable in their arguments, and we refer to the paper by Ponosov et al. [38, Thm. 1] for more details on the existence and uniqueness of solutions to the initial value problem (3.1)–(3.2). See also the book by Hale and Lunel [18].

Definition 3.1. A scalar-valued kernel, $\alpha : \mathbb{R}_{\geq 0} \rightarrow \mathbb{R}_{\geq 0}$, is regular if it satisfies the following properties.

1. It is non-negative and bounded, i.e., $0 \leq \alpha(t) \leq K$ for all $t \in \mathbb{R}_{\geq 0}$ and for some finite $K \in \mathbb{R}_{> 0}$.
2. It is continuous, i.e., for all $\epsilon \in \mathbb{R}_{> 0}$ and $t \in \mathbb{R}_{\geq 0}$, there exists a $\delta \in \mathbb{R}_{> 0}$ such that $|\alpha(s) - \alpha(t)| < \epsilon$ for all $s \in \mathbb{R}_{\geq 0}$ satisfying $|s - t| < \delta$.
3. It is normalized such that

$$(3.3) \quad \int_0^{\infty} \alpha(t) dt = 1.$$

For a given system of DDEs with distributed time delays, each element of α may not satisfy (3.3). However, as they are assumed to be nonzero and non-negative, it is straightforward to normalize them. Next, we present a few well-known corollaries about the steady states of (3.1b)–(3.2) and their stability.

Corollary 3.2. *A state $\bar{x} \in \mathbb{R}^{n_x}$ is a steady state of the system (3.1b)–(3.2) if*

$$(3.4) \quad 0 = f(\bar{x}, \bar{z}), \quad \bar{z} = \bar{r} = h(\bar{x}).$$

Proof. In steady state, $x(t) = \bar{x}$ for all t . Consequently, $r(t) = \bar{r} = h(\bar{x})$ and

$$(3.5) \quad z(t) = \int_{-\infty}^t \alpha(t-s) \odot \bar{r} \, ds = \int_{-\infty}^t \alpha(t-s) \, ds \odot \bar{r} = \bar{r},$$

for all t , where we have used the property (3.3) of each element of α . ■

Corollary 3.3. *The system (3.1b)–(3.2) is locally asymptotically stable around a steady state, \bar{x} , satisfying (3.4) if $\operatorname{Re} \lambda < 0$ for all $\lambda \in \mathbb{C}$ that satisfy the characteristic equation*

$$(3.6) \quad \det \left(F - \lambda I + G \int_0^\infty e^{-\lambda s} \operatorname{diag} \alpha(s) \, ds H \right) = 0,$$

where $I \in \mathbb{R}^{n_x \times n_x}$ is an identity matrix. The matrices $F \in \mathbb{R}^{n_x \times n_x}$, $G \in \mathbb{R}^{n_x \times n_z}$, and $H \in \mathbb{R}^{n_z \times n_x}$ are the Jacobians of the right-hand side function and the delay function evaluated in the steady state:

$$(3.7) \quad F = \frac{\partial f}{\partial x}(\bar{x}, \bar{z}), \quad G = \frac{\partial f}{\partial z}(\bar{x}, \bar{z}), \quad H = \frac{\partial h}{\partial x}(\bar{x}).$$

Proof. The linearized system corresponding to (3.1b)–(3.2) describes the evolution of the deviation variable $X : \mathbb{R} \rightarrow \mathbb{R}^{n_x}$:

$$(3.8) \quad \dot{X}(t) = FX(t) + G \int_{-\infty}^t \alpha(t-s) \odot HX(s) \, ds, \quad X(t) = x(t) - \bar{x}.$$

See, e.g., [12, 13, 34] for proofs of the condition (3.6) for asymptotic stability of the linearized system in (3.8). ■

4. Mixed Erlang approximation. In this section, we introduce the Erlang kernel and the Erlang mixture kernel, and we prove that the parameters in the latter can be chosen such that it converges to any regular kernel. Figure 1 shows examples of Erlang kernels and Erlang mixture kernels for different rate parameters and coefficients. For simplicity of the presentation, we only consider scalar kernels in this section.

Definition 4.1. *The m 'th order Erlang kernel, $\ell_m : \mathbb{R}_{\geq 0} \rightarrow \mathbb{R}_{\geq 0}$, with rate parameter $a \in \mathbb{R}_{> 0}$ is given by [26]*

$$(4.1) \quad \ell_m(t) = b_m t^m e^{-at}, \quad b_m = \frac{a^{m+1}}{m!},$$

where $b_m \in \mathbb{R}_{\geq 0}$ is a normalization constant, and $m \in \mathbb{N}_{\geq 0}$.

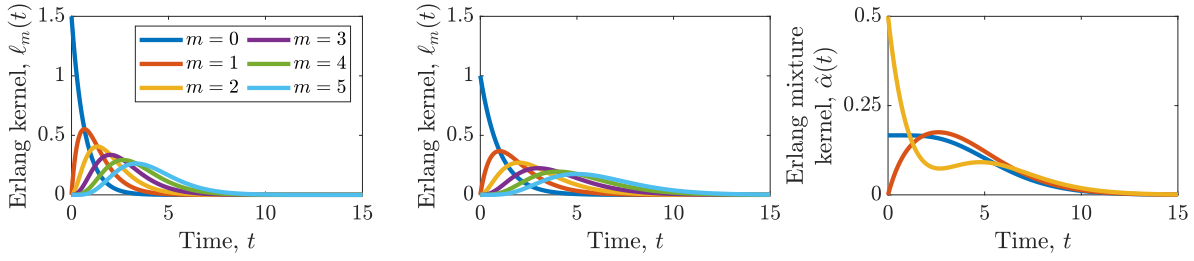


Figure 1. Erlang kernels for $a = 1.5$ (left) and $a = 1$ (middle) and $m = 0, \dots, 5$, and an Erlang mixture kernel (right) for $a = 1$, $M = 5$, and the following values of the coefficients. Blue: $c_m = 1/(M + 1)$. Red: $c_0 = 0$ and $c_m = 1/M$ for $m = 1, \dots, M$. Yellow: $c_0 = c_M = 1/2$ and $c_m = 0$ for $m = 1, \dots, M - 1$.

The normalization constant, b_m , is defined such that the integral of the Erlang kernel is one:

$$(4.2) \quad \int_0^{\infty} \ell_m(t) dt = 1.$$

Definition 4.2. The M 'th order Erlang mixture kernel, $\hat{\alpha} : \mathbb{R}_{\geq 0} \rightarrow \mathbb{R}_{\geq 0}$, with rate parameter $a \in \mathbb{R}_{> 0}$ and coefficients $c_m \in [0, 1]$ for $m = 0, \dots, M$ is given by

$$(4.3) \quad \hat{\alpha}(t) = \sum_{m=0}^M c_m \ell_m(t),$$

where $M \in \mathbb{N}_{\geq 0}$ and ℓ_m is an m 'th order Erlang kernel with rate parameter a . The coefficients must sum to one:

$$(4.4) \quad \sum_{m=0}^M c_m = 1.$$

A straightforward consequence of (4.2) and (4.4) is that

$$(4.5) \quad \int_0^{\infty} \hat{\alpha}(t) dt = 1.$$

4.1. Convergence. Next, we prove that an Erlang mixture kernel of infinite order converges to any regular kernel as the rate parameter, a , goes to infinity, for a specific choice of the coefficients $\{c_m\}_{m=0}^{\infty}$, which depends on the kernel that is being approximated. First, we define the Erlang mixture delta family, δ_a , which is shown in Figure 2 for different values of t and the rate parameter, a . Next, we prove a number of lemmas, and we will draw on the analogy of δ_a to the probability density function of a non-negative random variable, e.g., by determining its mean and variance. Finally, we present a general theorem about the approximation of regular kernels and use it to prove the above statement about the Erlang mixture kernel.

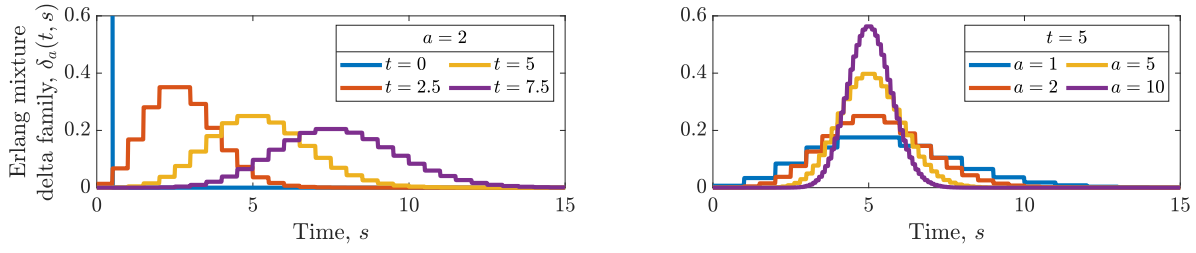


Figure 2. The Erlang mixture delta family for a fixed rate parameter, a , and different values of t (left) and for fixed t and different values of a (right). For $t = 0$ in the left figure, the value of δ_a is 2 for $s \in [0, 0.5)$ (see also Lemma 4.6).

Definition 4.3. An Erlang mixture delta family, $\delta_a : \mathbb{R}_{\geq 0} \times \mathbb{R}_{\geq 0} \rightarrow \mathbb{R}_{\geq 0}$, with rate parameter $a \in \mathbb{R}_{> 0}$ is the piecewise constant function

$$(4.6) \quad \delta_a(t, s) = \ell_m(t), \quad s \in [s_m, s_{m+1}), \quad s_m = m\Delta s, \quad \Delta s = 1/a,$$

where ℓ_m is an Erlang kernel of m 'th order with rate parameter a . The size of the intervals over which δ_a is piecewise constant is $\Delta s = s_{m+1} - s_m \in \mathbb{R}_{> 0}$ for all $m \in \mathbb{N}_{\geq 0}$, which depends on a , and in each interval, δ_a is equal to an Erlang kernel of different order.

Definition 4.4. The mean, $\mu : \mathbb{R}_{\geq 0} \rightarrow \mathbb{R}_{\geq 0}$, associated with a delta family, $\delta_a : \mathbb{R}_{\geq 0} \times \mathbb{R}_{\geq 0} \rightarrow \mathbb{R}_{\geq 0}$, is given by the integral

$$(4.7) \quad \mu(t) = \int_0^{\infty} \delta_a(t, s) s \, ds.$$

Definition 4.5. The variance, $\sigma^2 : \mathbb{R}_{\geq 0} \rightarrow \mathbb{R}_{\geq 0}$, associated with a delta family, $\delta_a : \mathbb{R}_{\geq 0} \times \mathbb{R}_{\geq 0} \rightarrow \mathbb{R}_{\geq 0}$, is given by the integral

$$(4.8) \quad \sigma^2(t) = \int_0^{\infty} \delta_a(t, s) (s - \mu(t))^2 \, ds,$$

or, equivalently, by

$$(4.9) \quad \sigma^2(t) = \mu_2(t) - \mu^2(t), \quad \mu_2(t) = \int_0^{\infty} \delta_a(t, s) s^2 \, ds,$$

where $\mu : \mathbb{R}_{\geq 0} \rightarrow \mathbb{R}_{\geq 0}$ is the mean given by (4.7).

Lemma 4.6. For $t = 0$, the Erlang mixture delta family is given by

$$(4.10) \quad \delta_a(0, s) = \begin{cases} a, & s \in [0, 1/a), \\ 0, & \text{otherwise.} \end{cases}$$

Proof. By direct substitution, $\ell_0(0) = a$ and $\ell_m(0) = 0$ for $m > 0$. Furthermore, by definition, $[s_0, s_1) = [0, 1/a)$. ■

Lemma 4.7. *The integral of an Erlang mixture delta family, $\delta_a : \mathbb{R}_{\geq 0} \times \mathbb{R}_{\geq 0} \rightarrow \mathbb{R}_{\geq 0}$, over all values of the second argument is one for all values of $a \in \mathbb{R}_{> 0}$ and $t \in \mathbb{R}_{\geq 0}$:*

$$(4.11) \quad \int_0^{\infty} \delta_a(t, s) \, ds = 1.$$

Proof. We substitute the expression for δ_a in (4.6) and simplify:

$$(4.12) \quad \begin{aligned} \int_0^{\infty} \delta_a(t, s) \, ds &= \sum_{m=0}^{\infty} \ell_m(t) \int_{s_m}^{s_{m+1}} 1 \, ds = \sum_{m=0}^{\infty} \ell_m(t) \Delta s = \sum_{m=0}^{\infty} \frac{(at)^m}{m!} a e^{-at} \frac{1}{a} \\ &= \sum_{m=0}^{\infty} \frac{(at)^m}{m!} e^{-at} = e^{-at} e^{at} = 1. \end{aligned}$$

Here, we have used (2.1). ■

Lemma 4.8. *Let $\delta_a : \mathbb{R}_{\geq 0} \times \mathbb{R}_{\geq 0} \rightarrow \mathbb{R}_{\geq 0}$ be an Erlang mixture delta family. Then, for all $t, s \in \mathbb{R}_{\geq 0}$, $\delta_a(t, s) \rightarrow 0$ as $a \rightarrow \infty$ if $s \neq t$.*

Proof. In the proof, we will use Stirling's approximation [43]: $\ln n! \approx n \ln n - n + \frac{1}{2} \ln 2\pi n$. The error of the approximation decreases with $1/n$. We will show that for given $\epsilon \in \mathbb{R}_{> 0}$ and for fixed s and t , it is possible to choose a sufficiently large that the inequality

$$(4.13) \quad \delta_a(t, s) = \ell_m(t) < \epsilon$$

is satisfied if $s \neq t$. For simplicity, we assume that a is chosen such that $m = as$ is integer. First, we assume that $t > 0$ and substitute ℓ_m and the value of m :

$$(4.14) \quad \frac{(at)^{as}}{(as)!} a e^{-at} < \epsilon.$$

Next, we take the logarithm on both sides and substitute Stirling's approximation:

$$(4.15a) \quad as \ln at - \ln(as)! + \ln a - at < \ln \epsilon,$$

$$(4.15b) \quad as \ln at - \left(as \ln as - as + \frac{1}{2} \ln 2\pi as \right) + \ln a - at < \ln \epsilon.$$

Finally, we rearrange terms:

$$(4.16) \quad a \left(s \left(\ln \frac{t}{s} + 1 \right) - t \right) + \frac{1}{2} \ln a < \ln \epsilon + \frac{1}{2} \ln 2\pi s.$$

For $s \neq t$, the factor of a in the first term is always negative, and it is always possible to satisfy the bound for sufficiently large a . This follows from the inequality $\ln x \leq x - 1$ for $x > 0$. In contrast, if $s = t$, the factor of a is zero, and the inequality is only satisfied if

$$(4.17) \quad \frac{1}{2} \ln a < \ln \epsilon + \frac{1}{2} \ln 2\pi s \quad \text{or} \quad a < 2\pi s \epsilon^2,$$

i.e., if a is bounded from above. For $t = 0$, $\delta_a(t, s)$ is only nonzero for $s < 1/a$ (see Lemma 4.6). Consequently, for a fixed $s \neq t$, it is always possible to choose a large enough that $\delta_a(t, s) = 0$. ■

Lemma 4.9. *An Erlang mixture delta family, $\delta_a : \mathbb{R}_{\geq 0} \times \mathbb{R}_{\geq 0} \rightarrow \mathbb{R}_{\geq 0}$, is non-decreasing in the second argument, s , when it is below the first argument, t , and non-increasing when it is above. Specifically, since δ_a is piecewise constant over intervals of size Δs , $\delta_a(t, s) \leq \delta_a(t, s + \Delta s)$ for $s < t$, and $\delta_a(t, s) \geq \delta_a(t, s + \Delta s)$ for $s \geq t$.*

Proof. Let $s \in [s_{m-1}, s_m)$. Then, $s + \Delta s \in [s_m, s_{m+1})$, and we derive a condition on m for δ_a to be non-decreasing:

$$(4.18) \quad \delta_a(t, s) \leq \delta_a(t, s + \Delta s).$$

We substitute the expressions for $\ell_{m-1}(t)$ and $\ell_m(t)$ on the left- and right-hand side, respectively,

$$(4.19) \quad \frac{(at)^{m-1}}{(m-1)!} ae^{-at} \leq \frac{(at)^m}{m!} ae^{-at},$$

and obtain the condition

$$(4.20) \quad m \leq at.$$

This corresponds to $s_m = m\Delta s = m/a \leq t$, and $s < s_m$ by assumption. Consequently, δ_a is non-decreasing in s for $s < t$, and the proof that δ_a is non-increasing in s for $s \geq t$ is analogous. ■

Lemma 4.10. *The mean, $\mu : \mathbb{R}_{\geq 0} \rightarrow \mathbb{R}_{\geq 0}$, associated with an Erlang mixture delta family, $\delta_a : \mathbb{R}_{\geq 0} \times \mathbb{R}_{\geq 0} \rightarrow \mathbb{R}_{\geq 0}$, with rate parameter a is given by*

$$(4.21) \quad \mu(t) = t + \frac{1}{2a},$$

and for finite $a \in \mathbb{R}_{>0}$, $\mu(t) > 0$ for all $t \in \mathbb{R}_{\geq 0}$.

Proof. We substitute the definition of δ_a in (4.6):

$$(4.22) \quad \mu(t) = \int_0^\infty \delta_a(t, s) s \, ds = \sum_{m=0}^\infty \ell_m(t) \int_{s_m}^{s_{m+1}} s \, ds.$$

Next, we write out the expression for the integral,

$$(4.23) \quad \begin{aligned} \int_{s_m}^{s_{m+1}} s \, ds &= \frac{1}{2}(s_{m+1}^2 - s_m^2) = \frac{1}{2}(s_{m+1} - s_m)(s_{m+1} + s_m) = \frac{1}{2}\Delta s((m+1) + m)\Delta s \\ &= \frac{2m+1}{2}\Delta s^2, \end{aligned}$$

and substitute into (4.22):

$$(4.24) \quad \begin{aligned} \mu(t) &= \sum_{m=0}^\infty \frac{(at)^m}{m!} ae^{-at} \frac{2m+1}{2} \Delta s^2 = t \sum_{m=1}^\infty \frac{(at)^{m-1}}{(m-1)!} e^{-at} + \frac{1}{2a} \sum_{m=0}^\infty \frac{(at)^m}{m!} e^{-at} \\ &= t + \frac{1}{2a}. \end{aligned}$$

Here, we have used the identity (2.1) and that $\Delta s = 1/a$. ■

Lemma 4.11. *The variance, $\sigma^2 : \mathbb{R}_{\geq 0} \rightarrow \mathbb{R}_{\geq 0}$, associated with an Erlang mixture delta family, $\delta_a : \mathbb{R}_{\geq 0} \times \mathbb{R}_{\geq 0} \rightarrow \mathbb{R}_{\geq 0}$, with rate parameter a is given by*

$$(4.25) \quad \sigma^2(t) = \frac{1}{a} \left(t + \frac{1}{12a} \right).$$

Proof. First, we write out the integral in the definition of μ_2 in (4.9):

$$(4.26) \quad \mu_2(t) = \int_0^\infty \delta_a(t, s) s^2 ds = \sum_{m=0}^\infty \ell_m(t) \int_{s_m}^{s_{m+1}} s^2 ds.$$

Next, we write out the integral of s^2 ,

$$(4.27) \quad \begin{aligned} \int_{s_m}^{s_{m+1}} s^2 ds &= \frac{1}{3} (s_{m+1}^3 - s_m^3) = \frac{1}{3} (s_{m+1} - s_m) (s_{m+1}^2 + s_{m+1}s_m + s_m^2) \\ &= \frac{1}{3} \Delta s ((m+1)^2 + (m+1)m + m^2) \Delta s^2 \\ &= \left(m(m-1) + 2m + \frac{1}{3} \right) \Delta s^3, \end{aligned}$$

and substitute it into the right-hand side of (4.26):

$$(4.28) \quad \mu_2(t) = \sum_{m=0}^\infty \frac{(at)^m}{m!} a e^{-at} \left(m(m-1) + 2m + \frac{1}{3} \right) \Delta s^3.$$

We simplify each of the three sums separately:

$$(4.29a) \quad \sum_{m=0}^\infty \frac{(at)^m}{m!} a e^{-at} m(m-1) \Delta s^3 = t^2 \sum_{m=2}^\infty \frac{(at)^{m-2}}{(m-2)!} e^{-at} = t^2,$$

$$(4.29b) \quad \sum_{m=0}^\infty \frac{(at)^m}{m!} a e^{-at} 2m \Delta s^3 = 2 \frac{t}{a} \sum_{m=1}^\infty \frac{(at)^{m-1}}{(m-1)!} e^{-at} = 2 \frac{t}{a},$$

$$(4.29c) \quad \sum_{m=0}^\infty \frac{(at)^m}{m!} a e^{-at} \frac{1}{3} \Delta s^3 = \frac{1}{3a^2} \sum_{m=0}^\infty \frac{(at)^m}{m!} e^{-at} = \frac{1}{3a^2}.$$

In all three cases, we have used the identity (2.1) and that $\Delta s = 1/a$. Finally, we substitute the resulting expression for μ_2 and the expression for the mean (4.21) into the definition of σ^2 in (4.9) and simplify:

$$(4.30) \quad \begin{aligned} \sigma^2(t) &= \mu_2(t) - \mu^2(t) = t^2 + 2 \frac{t}{a} + \frac{1}{3a^2} - \left(t + \frac{1}{2a} \right)^2 = t^2 + 2 \frac{t}{a} + \frac{1}{3a^2} - t^2 - \frac{1}{4a^2} - \frac{t}{a} \\ &= \frac{t}{a} + \frac{1}{12a^2}. \end{aligned} \quad \blacksquare$$

Lemma 4.12. Let $\delta : \mathbb{R}_{\geq 0} \times \mathbb{R}_{\geq 0} \rightarrow \mathbb{R}_{\geq 0}$ be an Erlang mixture delta family with mean $\mu : \mathbb{R}_{\geq 0} \rightarrow \mathbb{R}_{\geq 0}$ and rate parameter $a \in \mathbb{R}_{> 0}$. Then, the inequality

$$(4.31) \quad 1 - \int_{\mu(t)-\gamma}^{\mu(t)+\gamma} \delta_a(t, s) \, ds \leq \frac{\sigma^2(t)}{\gamma^2}$$

holds for all $\gamma \in \mathbb{R}_{> 0}$ that satisfy $\gamma \leq \mu(t)$.

Proof. This follows from Chebyshev's (or Markov's) well-known inequality in probability theory and the fact that $\mu(t) > 0$ for all $t \in \mathbb{R}_{\geq 0}$ and finite rate parameters, $a \in \mathbb{R}_{> 0}$. See, e.g., Lemma 4.1 in the book by Kallenberg [27]. ■

Lemma 4.13. Let $\delta : \mathbb{R}_{\geq 0} \times \mathbb{R}_{\geq 0} \rightarrow \mathbb{R}_{\geq 0}$ be an Erlang mixture delta family with rate parameter $a \in \mathbb{R}_{> 0}$. Then, for all $\gamma \in \mathbb{R}_{> 0}$ and $t \in \mathbb{R}_{\geq 0}$,

$$(4.32) \quad \int_{[t-\gamma]^+}^{t+\gamma} \delta_a(t, s) \, ds \rightarrow 1$$

as $a \rightarrow \infty$.

Proof. First, we assume that $t > 0$ and bound the integral from above and below using Lemma 4.7 and 4.12:

$$(4.33) \quad 1 - \frac{\sigma^2(t)}{\bar{\gamma}^2} \leq \int_{\mu(t)-\bar{\gamma}}^{\mu(t)+\bar{\gamma}} \delta_a(t, s) \, ds \leq \int_{[\mu(t)-\gamma]^+}^{\mu(t)+\gamma} \delta_a(t, s) \, ds \leq \int_0^{\infty} \delta_a(t, s) \, ds = 1.$$

Here, $\bar{\gamma} = \min\{t, \gamma\}$ such that the limits in the leftmost integral are non-negative. Consequently, since $\mu(t) \rightarrow t$ and $\sigma^2(t) \rightarrow 0$ as $a \rightarrow \infty$, the integral in (4.32) approaches one. Next, if $t = 0$, the integral in (4.32) is equal to one for all $a \geq 1/\gamma$. ■

Next, we prove the main results of this section. Theorem 4.14 is an adaptation of the theorem presented in Section 9.3 of the book by Korevaar [29] regarding the convergence of approximations based on delta families.

Theorem 4.14. Let $\delta_a : \mathbb{R}_{\geq 0} \times \mathbb{R}_{\geq 0} \rightarrow \mathbb{R}_{\geq 0}$ be a delta family parametrized by $a \in \mathbb{R}_{> 0}$ which satisfies the following conditions.

1. For all $\gamma \in \mathbb{R}_{> 0}$ and $t \in \mathbb{R}_{\geq 0}$,

$$(4.34) \quad \int_{[t-\gamma]^+}^{t+\gamma} \delta_a(t, s) \, ds \rightarrow 1$$

as $a \rightarrow \infty$.

2. For all $\gamma \in \mathbb{R}_{> 0}$ and for all $s \in \mathbb{R}_{\geq 0}$ satisfying $\gamma \leq |t - s| < \infty$, $\delta_a(t, s) \rightarrow 0$ uniformly as $a \rightarrow \infty$ for all $t \in \mathbb{R}_{\geq 0}$.
3. $\delta_a(t, s) \geq 0$ for all $t, s \in \mathbb{R}_{\geq 0}$ and $a \in \mathbb{R}_{> 0}$.

Furthermore, let $\alpha : \mathbb{R}_{\geq 0} \rightarrow \mathbb{R}_{\geq 0}$ be a regular kernel. Then, the approximation $\hat{\alpha} : \mathbb{R}_{\geq 0} \rightarrow \mathbb{R}_{\geq 0}$ given by

$$(4.35) \quad \hat{\alpha}(t) = \int_0^{\infty} \delta_a(t, s) \alpha(s) \, ds$$

converges (pointwise) to $\alpha(t)$ for all $t \in \mathbb{R}_{\geq 0}$ as $a \rightarrow \infty$.

Proof. First, we split the integral into two terms:

$$(4.36) \quad \hat{\alpha}(t) = \int_0^\infty \delta_a(t, s) \alpha(s) ds$$

$$(4.37) \quad = \underbrace{\int_{[t-\gamma]^+}^{t+\gamma} \delta_a(t, s) \alpha(s) ds}_{\mathcal{I}_1(t)} + \underbrace{\int_0^{[t-\gamma]^+} \delta_a(t, s) \alpha(s) ds + \int_{t+\gamma}^\infty \delta_a(t, s) \alpha(s) ds}_{\mathcal{I}_2(t)}.$$

Next, we add zero to the first term and split the integral:

$$(4.38) \quad \mathcal{I}_1(t) = \underbrace{\alpha(t) \int_{[t-\gamma]^+}^{t+\gamma} \delta_a(t, s) ds}_{\mathcal{I}_3(t)} + \underbrace{\int_{[t-\gamma]^+}^{t+\gamma} \delta_a(t, s) (\alpha(s) - \alpha(t)) ds}_{\mathcal{I}_4(t)}.$$

The second term, $\mathcal{I}_4(t)$, can be bounded through the continuity of α . Specifically, choose γ such that $|\alpha(s) - \alpha(t)| < \epsilon$ for $|s - t| < \gamma$. Then,

$$(4.39) \quad \mathcal{I}_4(t) < \epsilon \int_{[t-\gamma]^+}^{t+\gamma} \delta_a(t, s) ds < \epsilon.$$

Next, we prove that the term $\mathcal{I}_2(t) \rightarrow 0$ as $a \rightarrow \infty$. We bound \mathcal{I}_2 from above by substituting the supremum of δ_a , bounding the integrals by 1, and utilizing the non-negativity of α and δ_a :

$$(4.40) \quad \mathcal{I}_2(t) = \int_0^{[t-\gamma]^+} \delta_a(t, s) \alpha(s) ds + \int_{t+\gamma}^\infty \delta_a(t, s) \alpha(s) ds \leq \sup_{\substack{s \in \mathbb{R}_{\geq 0} \\ \gamma \leq |t-s| < \infty}} \delta_a(t, s).$$

Furthermore, we note that by assumption, the supremum of δ_a over values of s outside of an interval around t goes to zero as $a \rightarrow \infty$. We choose a large enough that $\mathcal{I}_2(t) < \epsilon$. Additionally, we choose a large enough that

$$(4.41) \quad 1 - \int_{[t-\gamma]^+}^{t+\gamma} \delta_a(t, s) ds < \epsilon.$$

Then,

$$(4.42) \quad |\mathcal{I}_3(t) - \alpha(t)| = \alpha(t) \left(1 - \int_{[t-\gamma]^+}^{t+\gamma} \delta_a(t, s) ds \right) < \alpha(t) \epsilon,$$

and by utilizing the above bounds, we can choose a sufficiently large that

$$(4.43) \quad \begin{aligned} |\hat{\alpha}(t) - \alpha(t)| &< |\mathcal{I}_1(t) - \alpha(t)| + \mathcal{I}_2(t) \\ &< |\mathcal{I}_3(t) - \alpha(t)| + \mathcal{I}_4(t) + \mathcal{I}_2(t) \\ &< (\alpha(t) + 2)\epsilon, \end{aligned}$$

for any $\epsilon \in \mathbb{R}_{>0}$. We have made repeated use of triangle equalities and the fact that the integrals $\mathcal{I}_i(t)$ for $i = 1, \dots, 4$ and $t \in \mathbb{R}_{\geq 0}$ are non-negative. To summarize, for any $\bar{\epsilon} \in \mathbb{R}_{>0}$, we can choose $\bar{a} \in \mathbb{R}_{>0}$ such that $|\hat{\alpha}(t) - \alpha(t)| < \bar{\epsilon}$ for all $a \geq \bar{a}$. ■

Theorem 4.15. Let $\hat{\alpha} : \mathbb{R}_{\geq 0} \rightarrow \mathbb{R}_{\geq 0}$ be an Erlang mixture kernel of infinite order with rate parameter $a \in \mathbb{R}_{> 0}$,

$$(4.44) \quad \hat{\alpha}(t) = \sum_{m=0}^{\infty} c_m \ell_m(t),$$

where the coefficients are given by

$$(4.45) \quad c_m = \int_{s_m}^{s_{m+1}} \alpha(s) ds, \quad m = 0, 1, \dots,$$

for $s_m = m\Delta s \in \mathbb{R}_{\geq 0}$ and $\Delta s = 1/a \in \mathbb{R}_{> 0}$. Furthermore, let $\alpha : \mathbb{R}_{\geq 0} \rightarrow \mathbb{R}_{\geq 0}$ be a regular kernel. Then, $\hat{\alpha}$ converges pointwise to α , i.e.,

$$(4.46) \quad \hat{\alpha}(t) \rightarrow \alpha(t)$$

as $a \rightarrow \infty$ for all $t \in \mathbb{R}_{\geq 0}$.

Proof. First, we prove that the Erlang mixture delta family δ_a satisfies the three properties of Theorem 4.14. The first property follows directly from Lemma 4.13. The second property follows from Lemma 4.8 and the monotonicity properties in Lemma 4.9, i.e., the convergence is uniform outside of an interval around t because δ_a is monotonically non-decreasing and non-increasing for values of s lower and higher than t , respectively. Finally, it is straightforward to verify the third property from Definition 4.1 and 4.3 because ℓ_m is the product of a monomial and an exponential function with non-negative arguments. Next, it follows from the definition of the Erlang mixture delta family, δ_a , that the approximation in (4.35) is an Erlang mixture kernel of infinite order,

$$(4.47) \quad \hat{\alpha}(t) = \int_0^{\infty} \delta_a(t, s) \alpha(s) ds = \sum_{m=0}^{\infty} \ell_m(t) \int_{s_m}^{s_{m+1}} \alpha(s) ds,$$

and that the coefficients are given by (4.45). ■

Corollary 4.16. The coefficients defined by (4.45) sum to one, i.e.,

$$(4.48) \quad \sum_{m=0}^{\infty} c_m = 1.$$

Proof. This is a straightforward consequence of the fact that, by assumption, the integral of α is one. We write out the sum of the coefficients:

$$(4.49) \quad \sum_{m=0}^{\infty} c_m = \sum_{m=0}^{\infty} \int_{s_m}^{s_{m+1}} \alpha(s) ds = \int_0^{\infty} \alpha(s) ds = 1. \quad \blacksquare$$

Remark 4.17. To the best of the author's knowledge, the result in Theorem 4.15 is novel, i.e., it has not been proven that the probability density function of an Erlang mixture distribution of infinite order converges pointwise to that of any non-negative random variable

with a density function that satisfies the regularity conditions in Definition 3.1. It has been proven [11, 49] that the cumulative distribution function of such an Erlang mixture distribution converges to that of any non-negative random variable (i.e., convergence in distribution has been proven). Furthermore, it is well-known that, according to Scheffé's lemma [45], the convergence of probability density functions implies convergence of cumulative distribution functions. However, the converse is only true if the probability density function is bounded and equicontinuous [7, 48]. Alternatively, the converse is also true if the probability density function converges uniformly [44]. However, it is outside the scope of the present work to further investigate these alternative proofs.

5. Approximate system of ordinary differential equations. In this section, we use the Erlang mixture approximation presented in Section 4 to approximate the multivariate kernel in the DDEs presented in Section 3, and we use the LCT to transform the resulting approximate system to ODEs. Furthermore, we describe the steady state equations for the approximate system of ODEs together with a stability criterion. Finally, we present a comparison of the stability criteria for the approximate and original system.

First, we approximate the system of DDEs (3.1b)–(3.2) by

$$(5.1a) \quad \dot{\hat{x}}(t) = f(\hat{x}(t), \hat{z}(t)),$$

$$(5.1b) \quad \hat{z}(t) = \int_{-\infty}^t \hat{\alpha}(t-s) \odot \hat{r}(s) ds,$$

$$(5.1c) \quad \hat{r}(t) = h(\hat{x}(t)),$$

where each element of the kernel $\hat{\alpha} : \mathbb{R}_{\geq 0}^{n_z} \rightarrow \mathbb{R}_{\geq 0}^{n_z}$ is an Erlang mixture kernel:

$$(5.2) \quad \hat{\alpha}_i(t) = \sum_{m=0}^{M_i} c_{m,i} \ell_{m,i}(t), \quad i = 1, \dots, n_z.$$

The subscript i on the Erlang kernels, $\ell_{m,i} : \mathbb{R}_{\geq 0} \rightarrow \mathbb{R}_{\geq 0}$, indicates that it depends on the i 'th rate parameter, $a_i \in \mathbb{R}_{>0}$. Furthermore, $\hat{x} : \mathbb{R} \rightarrow \mathbb{R}^{n_x}$ and $\hat{z}, \hat{r} : \mathbb{R} \rightarrow \mathbb{R}^{n_z}$ are approximations of x , z , and r , respectively.

Theorem 5.1. *The system of DDEs (5.1) with the kernel (5.2) is equivalent to the system of ODEs*

$$(5.3a) \quad \dot{\hat{x}}(t) = f(\hat{x}(t), \hat{z}(t)),$$

$$(5.3b) \quad \dot{\hat{Z}}(t) = A\hat{Z}(t) + B\hat{r}(t),$$

$$(5.3c) \quad \hat{z}(t) = C\hat{Z}(t),$$

$$(5.3d) \quad \hat{r}(t) = h(\hat{x}(t)),$$

where $\hat{Z} : \mathbb{R} \rightarrow \mathbb{R}^{M+n_z}$ contains auxiliary memory states, and $M = \sum_{i=1}^{n_z} M_i$. Furthermore,

the matrices $A \in \mathbb{R}^{M+n_z \times M+n_z}$, $B \in \mathbb{R}_{\geq 0}^{M+n_z \times n_z}$, $C \in [0, 1]^{n_z \times M+n_z}$ are block-diagonal:

$$(5.4a) \quad A = \text{blkdiag} \left(A^{(1)}, A^{(2)}, \dots, A^{(n_z)} \right),$$

$$(5.4b) \quad B = \text{blkdiag} \left(b^{(1)}, b^{(2)}, \dots, b^{(n_z)} \right),$$

$$(5.4c) \quad C = \text{blkdiag} \left(c^{(1)}, c^{(2)}, \dots, c^{(n_z)} \right).$$

The block-diagonal elements, $A^{(i)} \in \mathbb{R}^{(M_i+1) \times (M_i+1)}$, $b^{(i)} \in \mathbb{R}_{\geq 0}^{M_i+1 \times 1}$, and $c^{(i)} \in [0, 1]^{1 \times M_i+1}$, are given by

$$(5.5a) \quad A^{(i)} = a_i(L^{(i)} - I^{(i)}), \quad b^{(i)} = a_i e_1^{(i)}, \quad c^{(i)} = [c_{0,i} \quad c_{1,i} \quad \dots \quad c_{M_i,i}], \quad i = 1, \dots, n_z,$$

where $I^{(i)}, L^{(i)} \in \mathbb{R}^{M_i+1 \times M_i+1}$ are an identity matrix and a lower shift matrix, respectively, i.e., $L^{(i)}$ contains ones in the first subdiagonal and zeros elsewhere. Furthermore, the first element of $e_1^{(i)} \in \mathbb{R}^{M_i+1 \times 1}$ is one and the others are zero.

The transformation of the system of DDEs (5.1) to the system of ODEs (5.3) is standard [33, 38]. Therefore, we postpone the proof of Theorem 5.1 to Appendix A.

Theorem 5.2. A steady state, $\bar{x} \in \mathbb{R}^{n_x}$, of the approximate system of ODEs (5.3) satisfies

$$(5.6) \quad 0 = f(\bar{x}, \bar{z}), \quad \bar{z} = \bar{r} = h(\bar{x}),$$

i.e., it satisfies the same equations as a steady state of the original system (3.1b)–(3.2).

Proof. This result follows directly from the equivalence of the system of ODEs (5.3) to the system of DDEs (5.1) and Corollary 3.2. However, for completeness and to demonstrate some of the properties of the matrices A , B , and C , we prove it using direct computation. In steady state,

$$(5.7) \quad 0 = f(\bar{x}, \bar{z}), \quad 0 = A\bar{Z} + B\bar{r}.$$

Consequently,

$$(5.8) \quad \bar{Z} = -A^{-1}B\bar{r}, \quad \bar{z} = C\bar{Z} = -CA^{-1}B\bar{r}.$$

Note that each block-diagonal element of A is a lower bidiagonal matrix with nonzero elements in the diagonal and the first subdiagonal. Therefore, A is invertible. Specifically,

$$(5.9a) \quad A^{-1} = \text{blkdiag} \left(\left(A^{(1)} \right)^{-1}, \dots, \left(A^{(n_z)} \right)^{-1} \right),$$

$$(5.9b) \quad CA^{-1}B = \text{diag} \left(c^{(1)} \left(A^{(1)} \right)^{-1} b^{(1)}, \dots, c^{(n_z)} \left(A^{(n_z)} \right)^{-1} b^{(n_z)} \right).$$

The inverse of $A^{(i)}$ is a multiple of a lower triangular matrix of ones and the diagonal elements of (5.9b) can be derived analytically:

$$(5.10) \quad \left(A^{(i)} \right)^{-1} = \frac{-1}{a} \begin{bmatrix} 1 & & & \\ 1 & 1 & & \\ \vdots & & \ddots & \\ 1 & 1 & \dots & 1 \end{bmatrix}, \quad c^{(i)} \left(A^{(i)} \right)^{-1} b^{(i)} = - \sum_{m=0}^{M_i} c_{m,i} = -1.$$

Consequently, $-CA^{-1}B = I$ is an identity matrix, and

$$(5.11) \quad \bar{z} = \bar{r} = h(\bar{x}),$$

which concludes the proof. ■

Theorem 5.3. *The system (5.3) is locally asymptotically stable around a steady state, \bar{x} , that satisfies (5.6) if $\operatorname{Re} \lambda < 0$ for all eigenvalues $\lambda \in \mathbb{C}$ of the Jacobian matrix*

$$(5.12) \quad J = \begin{bmatrix} F & GC \\ BH & A \end{bmatrix},$$

where F , G , and H are the Jacobian matrices given by (3.7). Furthermore, the eigenvalues can be partitioned into two subsets. One of the subsets will contain M_i eigenvalues equal to $-a_i$ for $i = 1, \dots, n_z$, and the other will contain eigenvalues that satisfy the reduced characteristic equation

$$(5.13) \quad \det(F - \lambda I + GQ(\lambda)H) = 0, \quad Q_{ij}(\lambda) = \begin{cases} \sum_{m=0}^{M_i} c_{m,i} \left(\frac{a_i}{a_i + \lambda}\right)^{m+1}, & i = j, \\ 0, & i \neq j, \end{cases}$$

where $Q : \mathbb{C} \rightarrow \mathbb{C}^{n_z \times n_z}$.

Proof. An eigenvalue, λ , is a root of the characteristic polynomial

$$(5.14) \quad \det(J - \lambda I) = \det \begin{bmatrix} F - \lambda I & GC \\ BH & A - \lambda I \end{bmatrix} \\ = \det(F - \lambda I - GC(A - \lambda I)^{-1}BH) \det(A - \lambda I),$$

where we have used Schur's determinant formula (see, e.g., [55]). Next, we exploit the block-diagonal structure of A :

$$(5.15) \quad A - \lambda I = \operatorname{blkdiag}\left(A^{(1)} - \lambda I^{(1)}, \dots, A^{(n_z)} - \lambda I^{(n_z)}\right).$$

Consequently,

$$(5.16) \quad \det(A - \lambda I) = \prod_{i=1}^{n_z} \det(A^{(i)} - \lambda I^{(i)}) = \prod_{i=1}^{n_z} (-1)^{M_i} (a_i + \lambda)^{M_i},$$

and $\lambda = -a_i$ is an eigenvalue with algebraic multiplicity M_i for $i = 1, \dots, n_z$. As the rate parameters, a_i , are positive, $A - \lambda I$ is invertible. Next, we consider the diagonal matrix

$$(5.17) \quad C(A - \lambda I)^{-1}B = \operatorname{diag}\left(c^{(1)} \left(A^{(1)} - \lambda I^{(1)}\right)^{-1} b^{(1)}, \dots, c^{(n_z)} \left(A^{(n_z)} - \lambda I^{(n_z)}\right)^{-1} b^{(n_z)}\right).$$

First, we rewrite the matrix

$$(5.18) \quad A^{(i)} - \lambda I^{(i)} = a_i \left(L^{(i)} - I^{(i)}\right) - \lambda I^{(i)} = -(a_i + \lambda) \left(\frac{-a_i}{a_i + \lambda} L^{(i)} + I^{(i)}\right).$$

Consequently, the inverse is

$$(5.19) \quad \left(A^{(i)} - \lambda I^{(i)}\right)^{-1} = \frac{-1}{a_i + \lambda} \begin{bmatrix} 1 & & & \\ \frac{a_i}{a_i + \lambda} & 1 & & \\ \vdots & & \ddots & \\ \left(\frac{a_i}{a_i + \lambda}\right)^{M_i} & \left(\frac{a_i}{a_i + \lambda}\right)^{M_i - 1} & \cdots & 1 \end{bmatrix},$$

as can be verified by direct calculation, and the diagonal elements of the matrix in (5.17) are

$$(5.20) \quad c^{(i)} \left(A^{(i)} - \lambda I^{(i)}\right)^{-1} b^{(i)} = - \sum_{m=0}^{M_i} c_{m,i} \left(\frac{a_i}{a_i + \lambda}\right)^{m+1} = -Q_{ii}(\lambda).$$

Finally, we substitute into the left determinant on the right-hand side of (5.14) and obtain

$$(5.21) \quad \det(F - \lambda I + GQ(\lambda)H) = 0. \quad \blacksquare$$

Alternative proof. For completeness, we demonstrate that the result can also be obtained from the equivalence between (5.1) and (5.3) and the stability criterion in Lemma 3.3. First, we write out the following integral for an Erlang kernel of order m with rate parameter a_i :

$$(5.22) \quad \int_0^\infty e^{-\lambda s} \ell_{m,i}(s) ds = b_{m,i} \int_0^\infty s^m e^{-(a_i + \lambda)s} ds = b_{m,i} \frac{m!}{(a_i + \lambda)^{m+1}} = \left(\frac{a_i}{a_i + \lambda}\right)^{m+1}.$$

This follows from the fact that the integral of an Erlang kernel of order m with rate parameter $a_i + \lambda$ is one. Next, we use this result to write out the following integral involving an Erlang mixture kernel of order M_i with rate parameter a_i :

$$(5.23) \quad \int_0^\infty e^{-\lambda s} \hat{\alpha}_i(s) ds = \sum_{m=0}^{M_i} c_{m,i} \int_0^\infty e^{-\lambda s} \ell_{m,i}(s) ds = \sum_{m=0}^{M_i} c_{m,i} \left(\frac{a_i}{a_i + \lambda}\right)^{m+1} = Q_{ii}(\lambda).$$

Consequently,

$$(5.24) \quad G \int_0^\infty e^{-\lambda s} \text{diag } \hat{\alpha}(s) ds H = G \text{diag} \left\{ \int_0^\infty e^{-\lambda s} \hat{\alpha}_i(s) ds \right\}_{i=1}^{n_z} H = GQ(\lambda)H,$$

and the characteristic equation (3.6) becomes

$$(5.25) \quad \det(F - \lambda I + GQ(\lambda)H) = 0. \quad \blacksquare$$

Next, we analyze the relation between the stability criterion from Theorem 5.3 for the approximate system of ODEs and the one from Theorem 3.3 for the original system of DDEs. The analysis is based on the piecewise constant approximation of decaying exponentials described in Lemma 5.4 and illustrated in Figure 3.

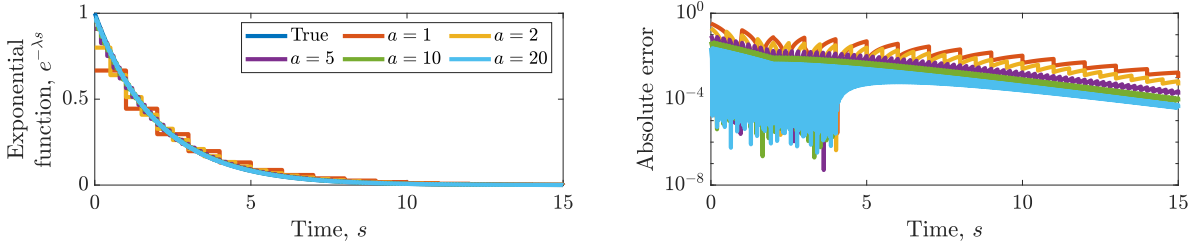


Figure 3. Left: The piecewise constant approximation (5.26) from Lemma 5.4 of a decaying exponential function, $e^{-\lambda s}$ for $\lambda = 1/2$ and different values of a . Right: The absolute error of the approximation.

Lemma 5.4. *The approximation*

$$(5.26) \quad e^{-\lambda s} \approx \left(\frac{a}{a + \lambda} \right)^{m+1}, \quad s \in [s_m, s_{m+1}), \quad s_m = m\Delta s, \quad \Delta s = 1/a,$$

converges as $a \rightarrow \infty$ for all $s, \lambda \in \mathbb{R}_{\geq 0}$.

Proof. First, we note that

$$(5.27) \quad \frac{a}{a + \lambda} = 1 - \frac{\lambda}{a + \lambda}, \quad \left(1 - \frac{\lambda}{a + \lambda} \right)^{m+1} \approx e^{-(m+1)\frac{\lambda}{a + \lambda}},$$

where the approximation is obtained by truncating the sum in (2.1) after the two first terms. It is valid for small arguments, and $\lambda/(a + \lambda) \rightarrow 0$ as $a \rightarrow \infty$. Furthermore, $m + 1 = s_{m+1}/\Delta s \approx as$ such that

$$(5.28) \quad e^{-(m+1)\frac{\lambda}{a + \lambda}} \approx e^{-\frac{a}{a + \lambda}\lambda s} \rightarrow e^{-\lambda s}$$

as $a \rightarrow \infty$. For $\lambda = 0$, the approximation is exact for all nonzero values of a . ■

Theorem 5.5. *For infinite-order Erlang mixture approximations of the elements of the kernel, α , as described in Theorem 4.15, the reduced characteristic function in (5.13) converges to the characteristic function in (3.6) as $a_i \rightarrow \infty$ for $i = 1, \dots, n_z$.*

Proof. First, we approximate the exponential function in (3.6) by

$$(5.29) \quad e^{-\lambda s} \approx \left(\frac{a_i}{a_i + \lambda} \right)^{m+1}, \quad s \in [s_m, s_{m+1}), \quad s_m = m\Delta s, \quad \Delta s = 1/a_i,$$

for the i 'th kernel. Next, we consider the integral in (3.6) for the i 'th element of α and substitute the approximation:

$$(5.30) \quad \int_0^\infty e^{-\lambda s} \alpha_i(s) ds \approx \sum_{m=0}^{\infty} \left(\frac{a_i}{a_i + \lambda} \right)^{m+1} \int_{s_m}^{s_{m+1}} \alpha_i(s) ds = \sum_{m=0}^{\infty} c_{m,i} \left(\frac{a_i}{a_i + \lambda} \right)^{m+1} = Q_{ii}(\lambda).$$

The coefficients were defined in (4.45) in Theorem 4.15. Consequently, as the approximation of the exponential function in (5.29) converges as $a_i \rightarrow \infty$ for $i = 1, \dots, n_z$,

$$(5.31) \quad \det(F - \lambda I + GQ(\lambda)H) \rightarrow \det\left(F - \lambda I + G \int_0^\infty e^{-\lambda s} \text{diag } \alpha(s) \, ds H\right),$$

as well, which concludes the proof. ■

Corollary 5.6. *If $\lambda = 0$ is an eigenvalue of the Jacobian matrix J in (5.12), it is also a solution to the characteristic equation (3.6).*

Proof. As the rate parameters, a_i , are positive for $i = 1, \dots, n_z$, an eigenvalue of zero must be a root of the reduced characteristic equation in (5.13), i.e., it is not an eigenvalue of A . Furthermore,

$$(5.32) \quad Q_{ii}(0) = \sum_{m=0}^{M_i} c_{m,i} = 1,$$

i.e., $Q(0)$ is an identity matrix. Consequently, for an eigenvalue of zero,

$$(5.33) \quad \det(F + GH) = 0.$$

Similarly, if $\lambda = 0$, the characteristic equation (3.6) becomes

$$(5.34) \quad \det\left(F + G \int_0^\infty \text{diag } \alpha(s) \, ds H\right) = \det(F + GH) = 0,$$

which, as we have just shown, is satisfied. ■

6. Algorithm. In this section, we describe an algorithm for determining the coefficients and the rate parameter in an M 'th order Erlang mixture approximation of a regular kernel, $\alpha : \mathbb{R}_{\geq 0} \rightarrow \mathbb{R}_{\geq 0}$, for given $M \in \mathbb{N}_{\geq 0}$. For simplicity, we only consider scalar kernels in this section. The algorithm consists of two steps: First, we identify a domain in which we approximate the kernel and then, we use a least-squares approach to determine the coefficients and the rate parameter. Furthermore, we describe a reference approach based on the theoretical expressions (4.45) for the coefficients. Finally, we describe the implementation of the algorithm and the simulation of the original DDEs (3.1b)–(3.2b) and the approximate system of ODEs (5.3).

6.1. Domain. In order to determine the approximation domain, we introduce $\beta : \mathbb{R}_{\geq 0} \rightarrow [0, 1]$ given by

$$(6.1) \quad \beta(t) = \int_0^t \alpha(s) \, ds,$$

which is analogous to the cumulative distribution function of a random variable with probability density function α . As α is non-negative, β is non-decreasing, and for a given threshold, $\epsilon \in \mathbb{R}_{>0}$, we choose $t_h \in \mathbb{R}_{\geq 0}$ as the solution to the equation $1 - \beta(t) = \epsilon$ and approximate α in the interval $[0, t_h]$. We use bisection to determine t_h approximately. We assume that

an initial interval, $[t_0^\ell, t_0^u]$, is available and that it contains the root, i.e., that $1 - \beta(t_0^\ell) > \epsilon$ and $1 - \beta(t_0^u) < \epsilon$. If that is not the case, the interval can be shifted or scaled such that it does. Next, the k 'th iteration has converged and an approximate solution has been found if $|1 - \beta(t_k^m) - \epsilon|$ is below a specified threshold, where $t_k^m = \frac{1}{2}(t_k^\ell + t_k^u)$ is the midpoint. Otherwise, the next iteration considers the lower half of the interval, $[t_{k+1}^\ell, t_{k+1}^u] = [t_k^\ell, t_k^m]$, if $1 - \beta(t_k^m) < \epsilon$. Similarly, if $1 - \beta(t_k^m) > \epsilon$, the next iteration considers the upper half of the interval, $[t_{k+1}^\ell, t_{k+1}^u] = [t_k^m, t_k^u]$.

Remark 6.1. If the function β given by (6.1) cannot be derived analytically for a given kernel, α , it can be approximated using numerical quadrature (e.g., with MATLAB's function `integral`).

Remark 6.2. The equation $1 - \beta(t) = \epsilon$ can also be solved using a gradient-based approach, e.g., Newton's method. However, $1 - \beta(t)$ rounds to zero in finite-precision arithmetic when t is too large, e.g., in a computer implementation. Consequently, Newton iterations may stall if an iterate happens to become too large.

6.2. Identify kernel parameters. For a given order, $M \in \mathbb{N}_{\geq 0}$, and $t_h \in \mathbb{R}_{\geq 0}$, the objective is to determine the values of the coefficients, $c_m \in [0, 1]$ for $m = 0, \dots, M$, and the rate parameter, $a \in \mathbb{R}_{> 0}$, that minimize the integral of the squared error,

$$(6.2) \quad \int_0^{t_h} (\alpha(t) - \hat{\alpha}(t))^2 dt,$$

while satisfying the constraint that the coefficients must sum to one. We approximate this integral by a left rectangle rule (such that the objective function includes $\alpha(0)$) with N rectangles, and we determine the coefficients and rate parameters by solving the inequality-constrained nonlinear program (NLP)

$$(6.3a) \quad \min_{\{c_m\}_{m=0}^M, a} \phi = \frac{1}{2} \sum_{k=0}^{N-1} (\alpha(t_k) - \hat{\alpha}(t_k))^2 \Delta t,$$

$$(6.3b) \quad \text{subject to} \quad \sum_{m=0}^M c_m = 1,$$

$$(6.3c) \quad 0 \leq c_m \leq 1, \quad m = 0, \dots, M,$$

$$(6.3d) \quad a_{\min} \leq a,$$

where the quadrature points are $t_k = k\Delta t$ for $k = 0, \dots, N-1$ and $a_{\min} \in \mathbb{R}_{> 0}$ is an arbitrary lower bound, which ensures that only positive values of a are feasible. Furthermore, the objective function involves the regular kernel, $\alpha : \mathbb{R}_{\geq 0} \rightarrow \mathbb{R}_{\geq 0}$, and the M 'th order Erlang mixture kernel, $\hat{\alpha} : \mathbb{R}_{\geq 0} \rightarrow \mathbb{R}_{\geq 0}$, with coefficients $\{c_m\}_{m=0}^M$ and rate parameter a , evaluated at the quadrature points.

6.2.1. Derivatives. Many algorithms for solving NLPs in the form (6.3) can benefit from analytical expressions for the first- and second-order derivative of the objective function. The

derivatives of the objective function are

$$(6.4a) \quad \frac{\partial \phi}{\partial v} = - \sum_{k=0}^{N-1} (\alpha(t_k) - \hat{\alpha}(t_k)) \frac{\partial \hat{\alpha}}{\partial v}(t_k) \Delta t,$$

$$(6.4b) \quad \frac{\partial^2 \phi}{\partial v \partial w} = - \sum_{k=0}^{N-1} \left((\alpha(t_k) - \hat{\alpha}(t_k)) \frac{\partial^2 \hat{\alpha}}{\partial v \partial w}(t_k) - \frac{\partial \hat{\alpha}}{\partial w}(t_k) \frac{\partial \hat{\alpha}}{\partial v}(t_k) \right) \Delta t,$$

where v and w represent either a or c_m . Furthermore, the first-order derivatives of the Erlang mixture kernel are

$$(6.5a) \quad \frac{\partial \hat{\alpha}}{\partial a}(t) = \sum_{m=0}^M c_m \frac{\partial \ell_m}{\partial a}(t),$$

$$(6.5b) \quad \frac{\partial \hat{\alpha}}{\partial c_k}(t) = \ell_k(t), \quad k = 0, \dots, M,$$

and the second-order derivatives are

$$(6.6a) \quad \frac{\partial^2 \hat{\alpha}}{\partial^2 a}(t) = \sum_{m=0}^M c_m \frac{\partial^2 \ell_m}{\partial^2 a}(t),$$

$$(6.6b) \quad \frac{\partial^2 \hat{\alpha}}{\partial a \partial c_k}(t) = \frac{\partial \ell_k}{\partial a}(t), \quad k = 0, \dots, M,$$

$$(6.6c) \quad \frac{\partial^2 \hat{\alpha}}{\partial c_k \partial c_n}(t) = 0, \quad k = 0, \dots, M, \quad n = 0, \dots, M.$$

Finally, the first- and second-order derivatives of the Erlang kernel with respect to the rate parameter are

$$(6.7a) \quad \frac{\partial \ell_m}{\partial a}(t) = \left(\frac{m+1}{a} - t \right) \ell_m(t), \quad m = 0, \dots, M,$$

$$(6.7b) \quad \frac{\partial^2 \ell_m}{\partial^2 a}(t) = \left(\frac{m+1}{a} - t \right) \frac{\partial \ell_m}{\partial a}(t) - \frac{m+1}{a^2} \ell_m(t), \quad m = 0, \dots, M.$$

6.3. Theoretical Erlang mixture approximation. We will compare the accuracy obtained with the least-squares approach described in Section 6.2 to that of a reference approach based on the theoretical values of the coefficients from Theorem 4.15. First, we determine the size of the approximation interval, t_h , such that $1 - \beta(t_h) \approx \epsilon$, e.g., using bisection as described in Section 6.1. Next, for a given order, M , we determine the rate parameter by $a = t_h/(M+1)$, and we use the theoretical expression (4.45) to compute the coefficients, c_m , for $m = 0, \dots, M$. In general, ϵ should be chosen to be small. Consequently, the coefficients will almost sum to one, and it is not necessary to scale them.

6.4. Implementation. We implement the evaluation of the objective function in the NLP (6.3) and its first- and second-order derivatives in C, and we use MATLAB's MEX interface to call the C routines from MATLAB. Furthermore, we use MATLAB's `fmincon` to

approximate the solution to the NLP, and we provide analytical first- and second-order derivatives. We exploit that $\alpha_m(t) = (at/m)\alpha_{m-1}(t)$ for $m = 1, \dots, M$ where $\alpha_0(t) = ae^{-at}$ is less prone to rounding errors than a straightforward evaluation of the expression (4.1) in the definition, and we use either double or long double precision when evaluating the Erlang kernels, the Erlang mixture kernels, and their derivatives. We simulate the approximate system of ODEs (5.3) using either MATLAB's `ode45` or `ode15s`, and depending on the order of the Erlang mixture kernel, we implement the matrices A , B , and C as either dense or sparse. Furthermore, we provide the analytical Jacobian of the right-hand side function of the approximate system of ODEs (5.3) to the simulator. We implement the numerical method for non-stiff DDEs described in Appendix B.1 in both MATLAB and C (with a MEX interface). The numerical method from Appendix B.2 is implemented in MATLAB, we use `fsolve` to solve the residual equations, and we provide the analytical Jacobian. In all three implementations, the right-hand side function, f , the delay function, h , and the kernel, α , are evaluated in MATLAB. Finally, in Section 8, we carry out parallel simulations and kernel approximations using a high-performance computing cluster [14].

7. Numerical test of the accuracy. In this section, we construct a DDE in the form (3.1b)–(3.2) with a known solution and use it to investigate the accuracy of the Erlang mixture approximation and the numerical solution of the approximate system of ODEs (5.3). Furthermore, we assess the convergence rate of the two numerical methods for solving initial value problems in the form (3.1)–(3.2) described in Appendix B.

We consider a modified logistic differential equation with a forcing term in the form

$$(7.1) \quad \dot{x}(t) = \sigma x(t) \left(1 - \frac{z(t)}{\kappa}\right) + Q(t), \quad z(t) = \int_{-\infty}^t \alpha(t-s)x(s) ds.$$

Here, $x : \mathbb{R} \rightarrow \mathbb{R}_{\geq 0}$ is a population density, $z : \mathbb{R} \rightarrow \mathbb{R}_{\geq 0}$ is the memory state, $\sigma \in \mathbb{R}_{> 0}$ is the logistic growth rate, $\kappa \in \mathbb{R}_{> 0}$ is a carrying capacity, and $Q : \mathbb{R} \rightarrow \mathbb{R}$ is the forcing term. We choose the solution, $x^* : \mathbb{R} \rightarrow \mathbb{R}_{\geq 0}$, and the kernel, $\alpha : \mathbb{R}_{\geq 0} \rightarrow \mathbb{R}_{\geq 0}$, as

$$(7.2) \quad x^*(t) = 1 + e^{-\left(\frac{t}{\gamma}\right)^2}, \quad \alpha(t) = \frac{2}{\sqrt{\pi}}e^{-t^2}, \quad \beta(t) = \operatorname{erf}(t),$$

where $\gamma \in \mathbb{R}_{> 0}$ is a dilation parameter, $\beta : \mathbb{R}_{\geq 0} \rightarrow [0, 1]$ is derived from (6.1), and $\operatorname{erf} : \mathbb{R} \rightarrow [0, 1]$ is the error function. Consequently, the true memory state, $z^* : \mathbb{R} \rightarrow \mathbb{R}_{\geq 0}$, is

$$(7.3) \quad z^*(t) = 1 + \frac{\gamma}{\sqrt{\gamma^2 + 1}} e^{-\frac{t^2}{\gamma^2 + 1}} \left(1 + \operatorname{erf}\left(\frac{t}{\gamma\sqrt{\gamma^2 + 1}}\right)\right),$$

and the forcing term is chosen such that x^* in (7.2) is the solution:

$$(7.4) \quad Q(t) = \dot{x}^*(t) - \sigma x^*(t) \left(1 - \frac{z^*(t)}{\kappa}\right).$$

This is referred to as the *method of manufactured solutions* [42].

Remark 7.1. We choose x^* such that it is bounded away from zero because the system becomes unstable if the numerical approximation of the solution becomes negative. This can happen when the true solution is close to zero, in which case the numerical approximation may diverge.

Figure 4 shows the approximation errors for the state and the kernel:

$$(7.5) \quad E_x = \sum_{n=0}^{K_x-1} (\hat{x}(t_{n+1}) - x^*(t_{n+1}))^2 \Delta t, \quad E_\alpha = \sum_{k=0}^{K_\alpha-1} (\hat{\alpha}(t_k) - \alpha(t_k))^2 \Delta t.$$

Here, \hat{x} and $\hat{\alpha}$ denote the approximations. Note that the kernel error, E_α , is analogous to the objective function in (6.3a) but may contain a different number of terms. We have used the model parameter values $\sigma = 4 \text{ mo}^{-1}$ and $\kappa = 1 \text{ mo}$ and the dilation parameter $\gamma = 10 \text{ mo}$, and the initial and final times are $t_0 = 0 \text{ mo}$ and $t_f = 24 \text{ mo}$. When we determine the Erlang mixture approximation of a given order, M , we use $N = 10^2$ points in the objective function in (6.3a). Furthermore, we use a threshold of $\epsilon = 10^{-14}$ and a convergence tolerance of 10^{-15} to determine the approximation interval length, t_h . Finally, we solve the NLP (6.3) using MATLAB's `fmincon` with an optimality tolerance of 10^{-10} and a step size tolerance below machine precision, and we use double precision in the involved kernel evaluations. We also use the identified value of t_h in the reference approach described in Section 6.3. We use MATLAB's `ode45` with absolute and relative tolerances of 10^{-12} to simulate the approximate system of ODEs (5.3), and we use $K_x = 24 \cdot 10^3$ quadrature points to evaluate the state error in (7.5), which corresponds to a time step size of $\Delta t = 10^{-3} \text{ mo}$. Furthermore, we use $K_\alpha = 10^6$ quadrature points to evaluate the kernel error. For the results obtained with the numerical methods described in Appendix B, we use a memory horizon of $\Delta t_h = t_f - t_0 = 24 \text{ mo}$ and the above time step size, and for the method for stiff DDEs, we use a function tolerance of 10^{-12} and an optimality tolerance of 10^{-8} when we solve the involved residual equations with MATLAB's `fsolve`.

The results demonstrate that for this example, the Erlang mixture approximation obtained with the proposed least-squares approach is several orders of magnitude more accurate than the reference approach based on the theoretical expressions for the coefficients. In both cases, there is a high correlation between the error of the kernel and the error of the approximate state trajectory. The kernel and state error is higher for $M = 32$ than 16 because the objective function in the NLP (6.3) uses a coarser resolution in the rectangle rule than the error in (7.5). Finally, the state error decreases quadratically with the time step size for the two numerical methods described in Appendix B because the involved integral have been discretized with first-order methods and the error is squared in (7.5).

8. Numerical examples. In this section, we present two numerical examples that demonstrate how Erlang mixture approximations can be used to approximately analyze and simulate DDEs with distributed time delays. In the first example, we use the approximate system of ODEs (5.3) to perform a numerical bifurcation analysis of the modified logistic differential equation that was also considered in Section 7, and in the second example, we present a Monte Carlo simulation of a molten salt nuclear fission process, which is nonlinear, multivariate, and stiff. We use high orders, M , and strict tolerances in the numerical methods to mitigate any

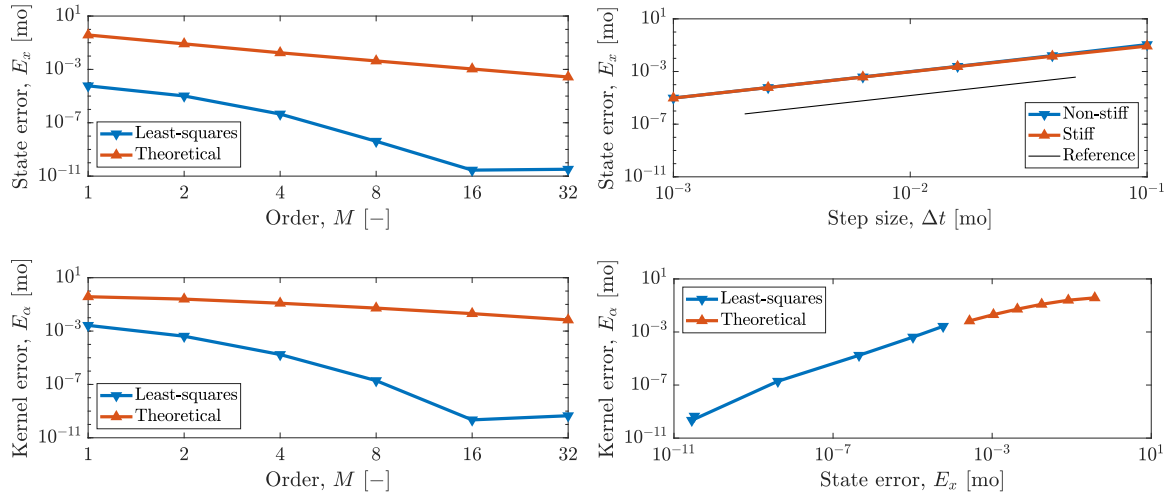


Figure 4. The state (top left) and kernel (bottom left) errors for Erlang mixture approximations of different orders, M , obtained with the proposed least-squares approach and the reference approach based on the theoretical expressions for the coefficients. The bottom right shows the state and kernel errors against each other, and the top right plot shows the state error obtained with the numerical approaches for non-stiff and stiff DDEs for different time step sizes, Δt . The black solid line is proportional to Δt^2 .

adverse effects on the results. However, in many practical contexts, lower orders and less restrictive tolerances can be used with limited effect on the accuracy (see also Section 7).

8.1. Modified logistic equation. We consider the modified logistic differential equation (7.1) where the forcing term is $Q(t) = 0$ and the kernel is

$$(8.1) \quad \alpha(t) = \gamma_1 F(t; \mu_1, \sigma_1) + \gamma_2 F(t; \mu_2, \sigma_2).$$

Here, $\gamma_1, \gamma_2 \in [0, 1]$ are weights, $\mu_1, \mu_2 \in \mathbb{R}$ are location parameters, $\sigma_1, \sigma_2 \in \mathbb{R}_{>0}$ are scale parameters, and $F : \mathbb{R}_{\geq 0} \times \mathbb{R} \times \mathbb{R}_{>0} \rightarrow \mathbb{R}_{\geq 0}$ is given by the probability density function of a folded normal distribution (i.e., it is a folded normal kernel):

$$(8.2) \quad F(t; \mu_i, \sigma_i) = \frac{\exp\left(-\frac{1}{2} \left(\frac{t-\mu_i}{\sigma_i}\right)^2\right) + \exp\left(-\frac{1}{2} \left(\frac{t+\mu_i}{\sigma_i}\right)^2\right)}{\sqrt{2\pi} \sigma_i}, \quad i = 1, 2.$$

Furthermore, we derive β in (6.1) analytically.

We use the parameter values in Table 1, and the initial state is $x(t) = 0.9$ for $t \leq t_0$. We use the same parameters as in Section 7 to identify Erlang mixture kernels of order $M = 100$ in the bifurcation analysis with respect to the logistic growth rate, σ , and $M = 350$ in the analysis with respect to the kernel parameter μ_2 . In Figure 5, the first row shows the eigenvalues of the Jacobian of the right-hand side function in the approximate system of ODEs (5.3). For completeness, we consider a very large range of values for σ , but for numerical reasons, we have not been able to investigate larger values of μ_2 . The second row shows the largest real part of the eigenvalues and when the parameters become sufficiently large, the steady state $\bar{x} = \kappa$ becomes unstable. The two bottom rows show simulations obtained with the

Table 1

Values of the parameters in the modified logistic equation. For σ and μ_2 , only the nominal values are shown.

Model, kernel, and simulation parameters									
σ [1/mo]	κ [-]	γ_1 [-]	γ_2 [-]	μ_1 [mo]	μ_2 [mo]	σ_1 [mo]	σ_2 [mo]	t_0 [mo]	t_f [mo]
4	1	0.5	0.5	0.35	0.45	0.06	0.12	0	24

numerical method for non-stiff DDEs for the parameter values indicated in the second row (the colors match). We use a memory horizon of $\Delta t_h = t_f - t_0 = 24$ mo and 10,000 time steps. In both cases, the stability analysis based on the approximate set of ODEs (5.3) accurately predicts when the steady state is stable, marginally stable (where the largest real part of the eigenvalues is equal to zero), and unstable. For large values of σ , a limit cycle appears whereas for large values of μ_2 , the population density oscillates unstably. Figure 6 shows the identified kernels, the corresponding error, and the coefficients for different values of μ_2 . There is a similarity between the coefficients and the shape of the approximated kernel, e.g., in terms of bimodality. Furthermore, as μ_2 increases, more sharp spikes occur in the coefficients.

8.2. Nuclear fission. Next, we consider a point reactor kinetics model of a molten salt nuclear fission reactor [15, 52] where the molten salt is circulated through a heat exchanger outside of the reactor core. The model describes 1) the concentrations of $N_g = 6 \in \mathbb{N}$ neutron precursor groups, $C_i : \mathbb{R} \rightarrow \mathbb{R}_{\geq 0}$ for $i = 1, \dots, N_g$, which emit delayed neutrons, 2) the concentration of neutrons, $C_n : \mathbb{R} \rightarrow \mathbb{R}_{\geq 0}$ for $n = N_g + 1 \in \mathbb{N}$, and 3) the reactivity, $\rho : \mathbb{R} \rightarrow \mathbb{R}$, which represents the relative number of neutrons created per fission event:

$$(8.3a) \quad \dot{C}_i(t) = (C_{i,in}(t) - C_i(t))D + R_i(t), \quad \dot{C}_n(t) = R_n(t), \quad \dot{\rho}(t) = -\kappa H C_n(t).$$

The dilution rate, $D \in \mathbb{R}_{\geq 0}$, is the ratio between the volumetric inlet and outlet flow rate and the reactor core volume, $\kappa \in \mathbb{R}_{\geq 0}$ is a proportionality constant, and $H \in \mathbb{R}_{\geq 0}$ is the ratio between the power production proportionality constant and the heat capacity of the reactor core. Furthermore, the production rate $R : \mathbb{R} \rightarrow \mathbb{R}^n$ is defined in terms of the stoichiometric matrix $S \in \mathbb{R}^{N_r \times n}$ where $N_r = n \in \mathbb{N}$ is the number of reactions and $r : \mathbb{R} \rightarrow \mathbb{R}_{\geq 0}^{N_r}$ is a vector of reaction rates:

$$(8.4) \quad R(t) = S^T(t)r(t), \quad S(t) = \begin{bmatrix} -1 & & & 1 \\ & \ddots & & \vdots \\ & & -1 & 1 \\ \beta_1 & \cdots & \beta_{N_g} & \rho(t) - \beta \end{bmatrix}, \quad r(t) = \begin{bmatrix} \lambda_1 C_1(t) \\ \vdots \\ \lambda_{N_g} C_{N_g}(t) \\ C_n(t)/\Lambda \end{bmatrix}.$$

Here, $\lambda_i, \beta_i, \Lambda \in \mathbb{R}_{\geq 0}$ for $i = 1, \dots, N_g$ are decay constants, delayed neutron fractions (i.e., the relative number of neutrons that are generated from the decay of neutron precursors), and the mean neutron generation time, respectively, and $\beta \in \mathbb{R}_{\geq 0}$ is the sum of β_i for $i = 1, \dots, N_g$. The inlet concentration, $C_{i,in} : \mathbb{R} \rightarrow \mathbb{R}_{\geq 0}$, is the memory state given by

$$(8.5) \quad C_{i,in}(t) = \int_{-\infty}^t \alpha_i(t-s)C_i(s) ds, \quad i = 1, \dots, N_g.$$

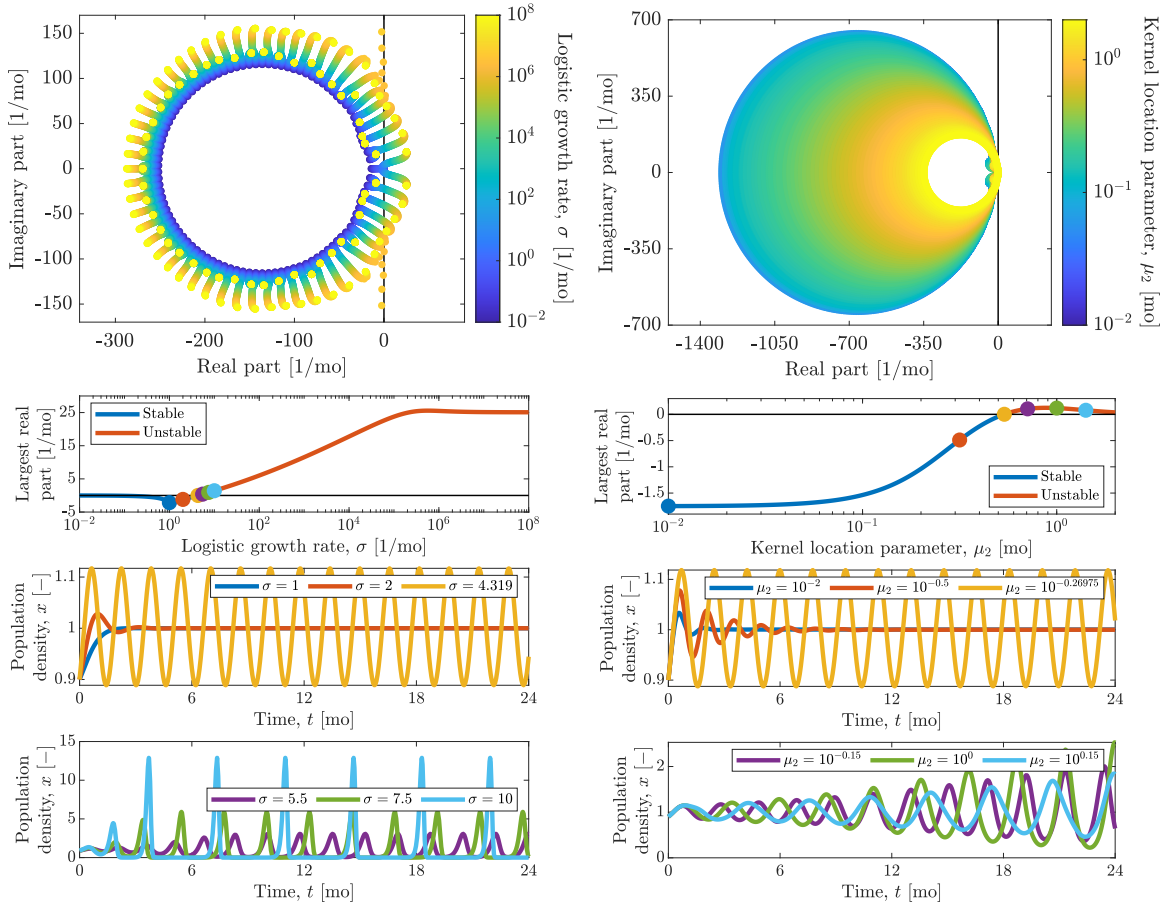


Figure 5. Bifurcation analysis with respect to the model parameter σ (left column) and the kernel parameter μ_2 (right column) for the modified logistic equation. First row: Eigenvalues. Second row: The largest real part of the eigenvalues. Third and bottom row: Simulations for selected parameter values (obtained with the numerical method described in Appendix B.1).

The kernels are described in Appendix C and represent 1) a nonuniform velocity profile in the external circulation of the molten salt (and neutron precursors) and 2) the (exponential) decay of the neutron precursors during the external circulation.

Table 2 shows the parameter values, which (except for D , μ_1 , and σ_1) are taken from [32]. We use $N = 1000$ points and an optimality tolerance of 10^{-10} in `fmincon` to identify Erlang mixture kernel approximations of order $M = 1000$. Furthermore, we use $\epsilon = 10^{-13}$ and a tolerance of 10^{-14} in the bisection algorithm, we use Matlab's `integral` with absolute and relative tolerances of 10^{-15} to approximate the integral in (6.1), and we use long double precision when evaluating the Erlang and Erlang mixture kernels. Figure 7 shows a Monte Carlo simulation for 1000 samples of κ drawn from a normal distribution with mean $3 \cdot 10^{-4}$ and standard deviation $7.5 \cdot 10^{-5}$. For brevity of the presentation, we omit the plots of the neutron precursor group concentrations. The initial states are $C_i(t) = 1 \text{ kmol/cm}^3$ for $i = 1, \dots, n$ and $\rho(t) = 1.1\beta$ for $t \leq t_0$, and we use an absolute and relative tolerance of 10^{-8} in `ode15s`

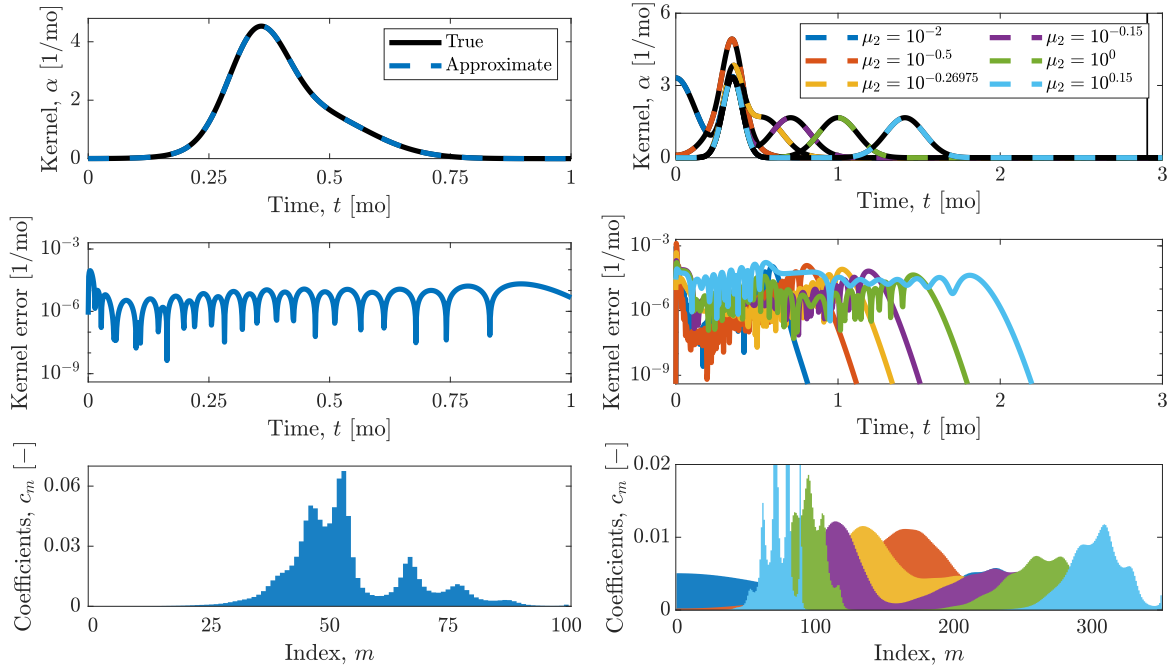


Figure 6. Top row: The true kernels and the corresponding Erlang mixture approximations for $M = 100$ (left) and $M = 350$ (right) obtained in connection with the bifurcation analysis shown in Figure 5. Middle row: The absolute errors of the kernel approximations. Bottom row: The coefficients in the Erlang mixture approximations. The colors are consistent across each column.

Table 2

Values of the parameters in the molten salt reactor model. For κ , only the nominal value is shown.

Decay constants [1/s]					
λ_1	λ_2	λ_3	λ_4	λ_5	λ_6
0.0124	0.0305	0.1110	0.3010	1.1300	3.0000
Delayed neutron fractions [-]					
β_1	β_2	β_3	β_4	β_5	β_6
0.00021	0.00141	0.00127	0.00255	0.00074	0.00027
Other model parameters					
Λ [s]	κ [1/K]	H [K cm ³ /s]	D [1/s]	μ_1 [s]	σ_1 [s]
$5 \cdot 10^{-5}$	$3 \cdot 10^{-4}$	0.05	2	2	0.1

to simulate the approximate system of ODEs (5.3). Furthermore, we supply the analytical Jacobian of the right-hand side function, and we represent it as a sparse matrix. The figure also shows the relative difference between the simulations obtained 1) as described above and 2) with the numerical method for stiff DDEs described in Appendix B.2 for the mean value of κ . The latter method uses a time step size of $6.25 \cdot 10^{-5}$ s, and the relative difference,

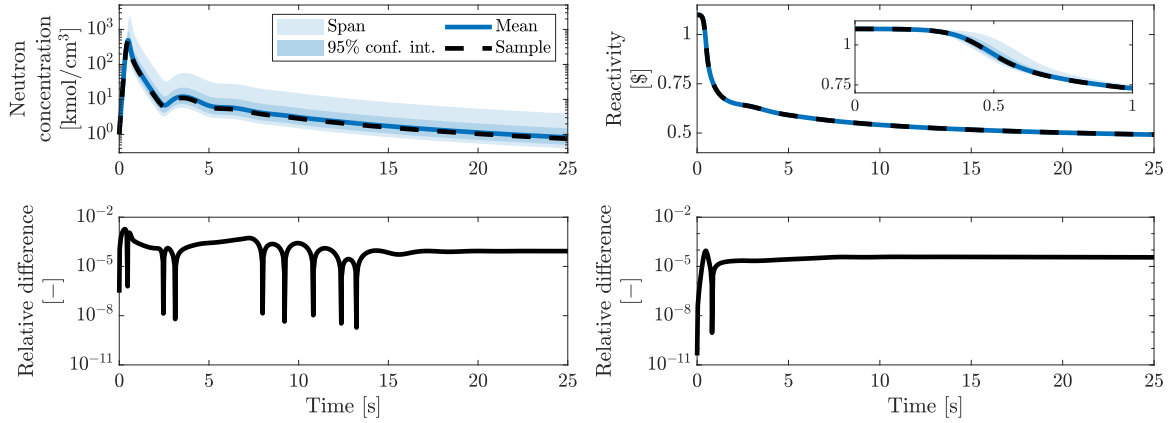


Figure 7. Monte Carlo simulation of the molten salt reactor model. Top row: The neutron concentration (left) and the reactivity (right). For each point in time, the span shows the interval of the minimum and maximum state, and the 95% confidence interval spans the 2.5 and 97.5 percentiles. The mean is computed pointwise, and the sample is the simulation corresponding to the mean value of κ . Bottom row: The pointwise relative error (8.6) between simulating the approximate ODEs (5.3) using `ode15s` and simulating the original DDEs using the numerical method for stiff DDEs described in Appendix B.2.

$E_{r,i} : \mathbb{R} \rightarrow \mathbb{R}_{\geq 0}$, in the i 'th state variable and n 'th time step is given by

$$(8.6) \quad E_{r,i}(t_n) = \frac{|\hat{x}_i(t_n) - x_i(t_n)|}{1 + |x_i(t_n)|}, \quad i = 1, \dots, n_x,$$

where \hat{x}_i is the approximate solution to the ODEs (5.3) and x_i is obtained with the numerical method for stiff DDEs. For each point in time, the 95% confidence intervals show the intervals from the 2.5 to the 97.5 percentiles and the span shows the interval of the minimum and maximum value of the states. For the neutron concentration, the confidence interval is almost symmetric (on the logarithmic axis) whereas the maximum is significantly higher above the mean than the minimum is below it. For the reactivity, the confidence interval and the span are hardly visible, and the simulation for the mean value of κ is indistinguishable from the pointwise mean. The maximum relative difference for all eight state variables is $2.14 \cdot 10^{-3}$. There are three main sources of error that affect this difference: 1) The kernel approximation error, 2) the error from using `ode15s` to simulate the approximate set of ODEs, and 3) the error of the numerical method described in Appendix B.2. If we use twice as large time steps in the latter, the maximum relative error is $4.28 \cdot 10^{-3}$, i.e., twice as large (results not shown). Therefore, we believe that the maximum relative difference would be further reduced by using smaller time step sizes, i.e., that the main source of error is that of the numerical method for stiff DDEs and not the Erlang mixture kernel approximation. However, due to large memory requirements, it has not been possible to further reduce the time step size. Finally, Figure 8 shows the Erlang mixture approximations of the kernels and the corresponding errors. It also shows the sum of folded normal kernels in (C.1) for the values of μ_1 and σ_1 shown in Table 2 and the coefficients in the Erlang mixture approximations. For some kernels, sharp spikes occur in the coefficients.

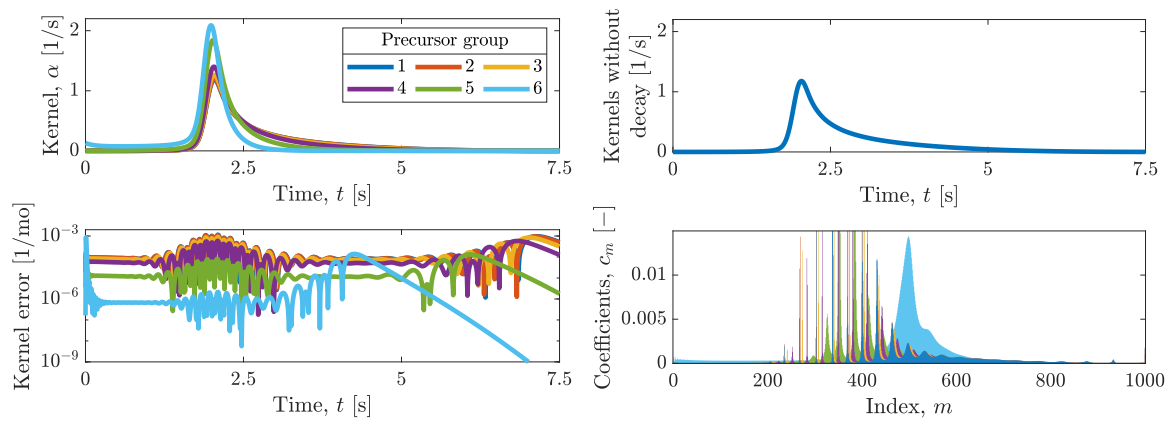


Figure 8. Left column: The Erlang mixture approximations of the kernels in (C.1) used in the Monte Carlo simulation shown in Figure 7 (top) and the corresponding approximation errors (bottom). Right column: The normalized sum of folded normal kernels in the expression (C.1) for the kernels (top), and the coefficients in the Erlang mixture kernel approximations. The colors are consistent across all but the top right figure.

9. Conclusions. In this paper, we propose an approximate approach for simulating and analyzing DDEs with distributed time delays based on conventional methods for ODEs. Specifically, we approximate the involved kernel by an Erlang mixture kernel and transform the resulting DDEs to ODEs using the LCT. Furthermore, we prove that if the kernel is continuous and bounded, an Erlang mixture kernel approximation of infinite order converges to the true kernel as the (common) rate parameter converges to infinity. Next, we compare the steady states of the original DDEs and the approximate system of ODEs as well as the corresponding stability criteria. Additionally, we propose an approach for determining optimal Erlang mixture approximations based on bisection and least-squares estimation, and we use a numerical example to demonstrate that its accuracy and rate of convergence can be higher than using the theoretical expressions for the coefficients obtained from the proof of convergence. Finally, we present two numerical examples that demonstrate the efficacy of the proposed approach, and we compare the results with those obtained by two numerical methods (for non-stiff and stiff systems) formulated directly for DDEs with distributed time delays.

Acknowledgments. The author would like to acknowledge many inspiring discussions on distributed time delays and delay differential equations with Prof. John Wyller from the Norwegian University of Life Sciences, Norway.

REFERENCES

- [1] I. AL-DARABSAH, S. A. CAMPBELL, AND B. RAHMAN, *Distributed delay and desynchronization in a neural mass model*, SIAM Journal on Applied Dynamical Systems, 23 (2024), pp. 3013–3051, <https://doi.org/10.1137/23M1618028>.
- [2] A. ALEKSANDROV, D. EFIMOV, AND E. FRIDMAN, *Analysis of homogeneous systems with distributed delay using averaging approach*, IFAC PapersOnLine, 56 (2023), pp. 174–179, <https://doi.org/10.1016/j.ifacol.2023.10.1565>.

- [3] A. ALEKSANDROV, D. EFIMOV, AND E. FRIDMAN, *On stability of nonlinear homogeneous systems with distributed delays having variable kernels*, Systems and Control Letters, 190 (2024), p. 105853, <https://doi.org/10.1016/j.sysconle.2024.105853>.
- [4] O. BAZIGHIFAN, E. M. ELABBASY, AND O. MOAAZ, *Oscillation of higher-order differential equations with distributed delay*, Journal of Inequalities and Applications, 2019 (2019), <https://doi.org/10.1186/s13660-019-2003-0>.
- [5] A. BELLEN, *Numerical methods for delay differential equations: Accuracy and stability problems*, IFAC Proceedings Volumes, 33 (2000), pp. 127–128, [https://doi.org/10.1016/S1474-6670\(17\)36928-8](https://doi.org/10.1016/S1474-6670(17)36928-8).
- [6] H. BERGLAND, P. MISHRA, P. A. PEDERSEN, A. PONOSSOV, AND J. WYLLER, *Time delays and pollution in an open-access fishery*, Natural Resource Modeling, 36 (2022), p. e12363, <https://doi.org/10.1111/nrm.12363>.
- [7] D. D. BOOS, *A converse to Scheffé's theorem*, The Annals of Statistics, 13 (1985), pp. 423–427, <https://doi.org/10.1214/aos/1176346604>.
- [8] T. CASSIDY, *Distributed delay differential equation representations of cyclic differential equations*, SIAM Journal of Applied Mathematics, 81 (2021), pp. 1742–1766, <https://doi.org/10.1137/20M1351606>.
- [9] T. CASSIDY, M. CRAIG, AND A. R. HUMPHRIES, *Equivalences between age structured models and state dependent distributed delay differential equations*, Mathematical Biosciences and Engineering, 16 (2019), pp. 5419–5450, <https://doi.org/10.3934/mbe.2019270>.
- [10] T. CASSIDY, P. GILLICH, A. R. HUMPHRIES, AND C. H. VAN DORP, *Numerical methods and hypoexponential approximations for gamma distributed delay differential equations*, IMA Journal of Applied Mathematics, 87 (2022), pp. 1043–1089, <https://doi.org/10.1093/imamat/hxac027>.
- [11] H. COSSETTE, D. LANDRIault, E. MARCEAU, AND K. MOUTANABBIR, *Moment-based approximation with mixed Erlang distributions*, Variance, 10 (2016), pp. 166–182.
- [12] J. M. CUSHING, *An operator equation and bounded solutions of integro-differential systems*, SIAM Journal on Mathematical Analysis, 6 (1975), pp. 433–445, <https://doi.org/10.1137/0506038>.
- [13] J. M. CUSHING, *Integrodifferential equations and delay models in population dynamics*, vol. 20 of Lectures Notes in Biomathematics, Springer, 1977, <https://doi.org/10.1007/978-3-642-93073-7>.
- [14] DTU COMPUTING CENTER, *DTU Computing Center resources*, 2025, <https://doi.org/10.48714/DTU.HPC.0001>.
- [15] J. J. DUDERSTADT AND L. J. HAMILTON, *Nuclear reactor analysis*, Wiley, 1976.
- [16] A. S. EREMIN, *Runge-Kutta methods for differential equations with distributed delays*, AIP Conference Proceedings, 2116 (2019), p. 140003, <https://doi.org/10.1063/1.5114130>.
- [17] L. GUERRINI, A. KRAWIEC, AND M. SZYDŁOWSKI, *Bifurcations in an economic growth model with a distributed time delay transformed to ODE*, Nonlinear Dynamics, 101 (2020), pp. 1263–1279, <https://doi.org/10.1007/s11071-020-05824-y>.
- [18] J. K. HALE AND S. M. V. LUNEL, *Introduction to functional differential equations*, vol. 99 of Applied Mathematical Sciences, Springer, 1993, <https://doi.org/10.1007/978-1-4612-4342-7>.
- [19] R. A. HORN AND C. R. JOHNSON, *Topics in matrix analysis*, Cambridge University Press, 1991, <https://doi.org/10.1017/CBO9780511840371>.
- [20] R. A. HORN AND C. R. JOHNSON, *Matrix Analysis*, Cambridge University Press, 2nd ed., 2012, <https://doi.org/10.1017/CBO9781139020411>.
- [21] S. HU, M. DUNLAVEY, S. GUZY, AND N. TEUSCHER, *A distributed delay approach for modeling delayed outcomes in pharmacokinetics and pharmacodynamics studies*, Journal of Pharmacokinetics and Pharmacodynamics, 45 (2018), pp. 285–308, <https://doi.org/10.1007/s10928-018-9570-4>.
- [22] C. HUANG AND S. VANDEWALLE, *An analysis of delay-dependent stability for ordinary and partial differential equations with fixed and distributed delays*, SIAM Journal on Scientific Computing, 25 (2004), pp. 1608–1632, <https://doi.org/10.1137/S1064827502409717>.
- [23] P. J. HURTADO AND A. S. KIROSINGH, *Generalizations of the 'Linear Chain Trick': Incorporating more flexible dwell time distributions into mean field ODE models*, Journal of Mathematical Biology, 79 (2019), pp. 1831–1883, <https://doi.org/10.1007/s00285-019-01412-w>.
- [24] P. J. HURTADO AND C. RICHARDS, *A procedure for deriving new ODE models: Using the generalized linear chain trick to incorporate phase-type distributed delay and dwell time assumptions*, Mathematics in Applied Sciences and Engineering, 1 (2020), pp. 412–424, <https://doi.org/10.5206/mase/10857>.
- [25] P. J. HURTADO AND C. RICHARDS, *Building mean field ODE models using the generalized linear chain*

- trick & Markov chain theory*, Journal of Biological Dynamics, 15 (2021), pp. S248–S272, <https://doi.org/10.1080/17513758.2021.1912418>.
- [26] O. C. IBE, *Fundamentals of applied probability and random processes*, Elsevier, 2nd ed., 2014, <https://doi.org/10.1016/C2013-0-19171-4>.
- [27] O. KALLENBERG, *Foundations of modern probability*, Springer, 2002, <https://doi.org/10.1007/978-3-030-61871-1>.
- [28] V. KOLMANOVSKII AND A. MYSHKIS, *Applied theory of functional differential equations*, vol. 85 of Mathematics and Its Applications, Springer, 1992, <https://doi.org/10.1007/978-94-015-8084-7>.
- [29] J. KOREVAAR, *Mathematical methods*, vol. 1, Academic Press, 1968.
- [30] W. KRZYZANSKI, *Ordinary differential equation approximation of gamma distributed delay model*, Journal of Pharmacokinetics and Pharmacodynamics, 46 (2019), pp. 53–63, <https://doi.org/10.1007/s10928-018-09618-z>.
- [31] W. KRZYZANSKI, S. HU, AND M. DUNLAVEY, *Evaluation of performance of distributed delay model for chemotherapy-induced myelosuppression*, Journal of Pharmacokinetics and Pharmacodynamics, 45 (2018), pp. 329–337, <https://doi.org/10.1007/s10928-018-9575-z>.
- [32] S. Q. B. LEITE, M. T. DE VILHENA, AND B. E. J. BODMANN, *Solution of the point reactor kinetics equations with temperature feedback by the ITS2 method*, Progress in Nuclear Energy, 91 (2016), pp. 240–249, <https://doi.org/10.1016/j.pnucene.2016.05.001>.
- [33] N. MACDONALD, *Time lags in biological models*, vol. 27 of Lectures Notes in Biomathematics, Springer, 1978, <https://doi.org/10.1007/978-3-642-93107-9>.
- [34] R. K. MILLER, *Asymptotic stability and perturbations for linear Volterra integrodifferential systems*, in Delay and Functional Differential Equations and Their Applications, K. Schmitt, ed., Academic Press, 1972, pp. 257–268, <https://doi.org/10.1016/B978-0-12-627250-5.50015-0>.
- [35] D. H. NEVERMANN AND C. GROS, *Mapping dynamical systems with distributed time delays to sets of ordinary differential equations*, Journal of Physics A: Mathematical and Theoretical, 56 (2023), p. 345702, <https://doi.org/10.1088/1751-8121/acea06>.
- [36] S.-I. NICULESCU AND K. GU, eds., *Advances in time-delay systems*, vol. 38 of Lecture Notes in Computational Science and Engineering, Springer, 2004, <https://doi.org/10.1007/978-3-642-18482-6>.
- [37] A. D. POLYANIN, V. G. SOROKIN, AND A. I. ZHUROV, *Delay ordinary and partial differential equations*, Advances in Applied Mathematics, CRC Press, 2023, <https://doi.org/10.1201/9781003042310>.
- [38] A. PONOSOV, A. SHINDIAPIN, AND J. J. MIGUEL, *The W-transform links delay and ordinary differential equations*, Functional Differential Equations, 9 (2002), pp. 437–469.
- [39] M. H. PROTTER AND C. B. MORREY, JR., *Intermediate Calculus*, Undergraduate Texts in Mathematics, Springer, 2nd ed., 1985, <https://doi.org/10.1007/978-1-4612-1086-3>.
- [40] B. RAHMAN, K. B. BLYUSS, AND Y. N. KYRYCHKO, *Dynamics of neural systems with discrete and distributed time delays*, SIAM Journal on Applied Dynamical Systems, 14 (2015), pp. 2069–2095, <https://doi.org/10.1137/15M1006398>.
- [41] T. K. S. RITSCHEL, *Numerical optimal control for distributed delay differential equations: A simultaneous approach based on linearization of the delayed variables*, 2024, <https://arxiv.org/abs/2410.15083>. Preprint.
- [42] P. J. ROACHE, *Code verification by the method of manufactured solutions*, Journal of Fluids Engineering, 124 (2002), pp. 4–10, <https://doi.org/10.1115/1.1436090>.
- [43] D. ROMIK, *Stirling’s approximation for $n!$: The ultimate short proof?*, The American Mathematical Monthly, 107 (2000), pp. 556–557, <https://doi.org/10.1080/00029890.2000.12005235>.
- [44] W. RUDIN, *Principles of mathematical analysis*, International Series in Pure and Applied Mathematics, McGraw-Hill, 3rd ed., 1976.
- [45] H. SCHEFFÉ, *A useful convergence theorem for probability distributions*, The Annals of Mathematical Statistics, 18 (1947), pp. 434–438, <https://doi.org/10.1214/aoms/1177730390>.
- [46] L. F. SHAMPINE AND S. THOMPSON, *Solving DDEs in MATLAB*, Applied Numerical Mathematics, 37 (2001), pp. 441–458, [https://doi.org/10.1016/S0168-9274\(00\)00055-6](https://doi.org/10.1016/S0168-9274(00)00055-6).
- [47] H. SMITH, *An introduction to delay differential equations with applications to the life sciences*, vol. 57 of Texts in Applied Mathematics, Springer, 2011, <https://doi.org/10.1007/978-1-4419-7646-8>.
- [48] T. J. SWEETING, *On a converse to Scheffé’s theorem*, The Annals of Statistics, 14 (1986), pp. 1252–1256, <https://doi.org/10.1214/aos/1176350065>.

- [49] H. C. TIJMS, *Stochastic models: An algorithmic approach*, Wiley Series in Probability and Statistics, Wiley, 1995.
- [50] S. TORKAMANI, E. A. BUTCHER, AND F. A. KHASAWNEH, *Parameter identification in periodic delay differential equations with distributed delay*, *Communications in Nonlinear Science and Numerical Simulation*, 18 (2013), pp. 1016–1026, <https://doi.org/10.1016/j.cnsns.2012.09.001>.
- [51] Y. WANG, Y. CONG, AND G. HU, *Delay-dependent stability of linear multistep methods for differential systems with distributed delays*, *Applied Mathematics and Mechanics*, 39 (2018), pp. 1837–1844, <https://doi.org/10.1007/s10483-018-2392-9>.
- [52] D. WOOTEN AND J. J. POWERS, *A review of molten salt reactor kinetics models*, *Nuclear Science and Engineering*, 191 (2018), pp. 203–230, <https://doi.org/10.1080/00295639.2018.1480182>.
- [53] X. YAN, R. BAUER, G. KOCH, J. SCHROPP, J. J. P. RUIXO, AND W. KRZYZANSKI, *Delay differential equations based models in NONMEM*, *Journal of Pharmacokinetics and Pharmacodynamics*, 48 (2021), pp. 763–802, <https://doi.org/10.1007/s10928-021-09770-z>.
- [54] Y. YUAN AND J. BÉLAIR, *Stability and Hopf bifurcation analysis for functional differential equation with distributed delay*, *SIAM Journal on Applied Dynamical Systems*, 10 (2011), pp. 551–581, <https://doi.org/10.1137/100794493>.
- [55] F. ZHANG, *The Schur complement and its applications*, vol. 4 of Numerical Methods and Algorithms, Springer, 2005, <https://doi.org/10.1007/b105056>.
- [56] G. ZHANG AND A. XIAO, *Exact and numerical stability analysis of reaction-diffusion equations with distributed delays*, *Frontiers of Mathematics in China*, 11 (2016), pp. 189–205, <https://doi.org/10.1007/s11464-015-0506-7>.
- [57] Z. ZHOU, *Statistical inference of distributed delay differential equations*, PhD thesis, University of Iowa, 2016, <https://doi.org/10.17077/etd.xgcf76n>.

Appendix A. Derivation of the linear chain trick.

Proof of Theorem 5.1. First, we introduce the auxiliary memory state $\hat{z}_{m,i} : \mathbb{R} \rightarrow \mathbb{R}$ given by

$$(A.1) \quad \hat{z}_{m,i}(t) = \int_{-\infty}^t \ell_{m,i}(t-s)\hat{r}_i(s) ds, \quad m = 0, \dots, M_i, \quad i = 1, \dots, n_z.$$

Next, we rewrite the expression for the memory state,

$$(A.2) \quad \hat{z}_i(t) = \int_{-\infty}^t \hat{\alpha}_i(t-s)\hat{r}_i(s) ds = \sum_{m=0}^{M_i} c_{m,i} \int_{-\infty}^t \ell_{m,i}(t-s)\hat{r}_i(s) ds = \sum_{m=0}^{M_i} c_{m,i} \hat{z}_{m,i}(t),$$

for $i = 1, \dots, n_z$. The time derivatives of the Erlang kernels are

$$(A.3a) \quad \dot{\ell}_{0,i}(t) = -a_i \ell_{0,i}(t), \quad i = 1, \dots, n_z,$$

$$(A.3b) \quad \dot{\ell}_{m,i}(t) = a_i(\ell_{m-1,i}(t) - \ell_{m,i}(t)), \quad m = 1, \dots, M_i, \quad i = 1, \dots, n_z,$$

and the normalization factor satisfies the recursion

$$(A.4) \quad b_{m,i} = \frac{a_i^{m+1}}{m!} = \frac{a_i}{m} \frac{a_i^m}{(m-1)!} = \frac{a_i}{m} b_{m-1,i}, \quad m = 1, \dots, M_i, \quad i = 1, \dots, n_z.$$

In order to derive differential equations for the auxiliary memory states, we use Leibniz' integral rule [39, Thm. 3, Chap. 8] to differentiate (A.1):

$$(A.5) \quad \dot{\hat{z}}_{m,i}(t) = \ell_{m,i}(0)\hat{r}_i(t) + \int_{-\infty}^t \dot{\ell}_{m,i}(t-s)\hat{r}_i(s) ds, \quad m = 0, \dots, M_i, \quad i = 1, \dots, n_z.$$

Next, we use the time derivatives of the Erlang kernels and the fact that

$$(A.6) \quad \ell_{m,i}(0) = \begin{cases} a_i, & \text{for } m = 0, \\ 0, & \text{for } m = 1, \dots, M_i, \end{cases} \quad i = 1, \dots, n_z,$$

to obtain the differential equations

$$(A.7a) \quad \dot{\hat{z}}_{0,i}(t) = a_i(\hat{r}_i(t) - \hat{z}_{0,i}(t)),$$

$$(A.7b) \quad \dot{\hat{z}}_{m,i}(t) = a_i(\hat{z}_{m-1,i}(t) - \hat{z}_{m,i}(t)), \quad m = 1, \dots, M_i.$$

Finally, by introducing the vector of all memory states,

$$(A.8) \quad \hat{Z} = \begin{bmatrix} \hat{z}_{0,0} \\ \hat{z}_{1,0} \\ \vdots \\ \hat{z}_{M_{n_z}, n_z} \end{bmatrix},$$

the system of DDEs (5.1) can be transformed to the system of ODEs (5.3). ■

Corollary A.1. *When the approximate system of ODEs (5.3) is in the steady state $\bar{x} \in \mathbb{R}^{n_x}$, the memory states are*

$$(A.9) \quad \bar{z}_i = \bar{z}_{m,i} = \bar{r}_i = h_i(\bar{x}), \quad m = 0, \dots, M_i, \quad i = 1, \dots, n_z.$$

Similarly, if the initial state function, $x_0 : \mathbb{R} \rightarrow \mathbb{R}^{n_x}$, is constant, the initial memory states are given by

$$(A.10) \quad \hat{z}_i(t_0) = \hat{z}_{m,i}(t_0) = \hat{r}_i(t_0) = h_i(x_0), \quad m = 0, \dots, M_i, \quad i = 1, \dots, n_z.$$

Proof. Both results follow directly from the fact that the integral of an Erlang kernel is one and that the coefficients sum to one. First, we consider the memory states in steady state:

$$(A.11) \quad \bar{z}_{m,i} = \bar{r}_i \int_{-\infty}^t \ell_{m,i}(t-s) ds = \bar{r}_i, \quad m = 0, \dots, M_i, \quad i = 1, \dots, n_z.$$

This holds for all $t \in \mathbb{R}$. Furthermore,

$$(A.12) \quad \bar{z}_i = \sum_{m=0}^{M_i} c_{m,i} \bar{z}_{m,i} = \bar{r}_i \sum_{m=0}^{M_i} c_{m,i} = \bar{r}_i, \quad i = 1, \dots, n_z.$$

The proof is analogous for the case where the initial state function is constant. ■

Appendix B. Numerical simulation. In this appendix, we present two numerical methods for simulating DDEs with distributed time delays, i.e., for approximating the solution to initial value problems in the form (3.1)–(3.2). The first is intended for non-stiff systems, and it uses Euler's explicit method to discretize the differential equations and a left rectangle rule to

discretize the integral in the convolution in (3.2a). In contrast, the second is intended for stiff systems, and it uses Euler's implicit method and a right rectangle rule to discretize the differential equations and the integral, respectively. In both cases, we truncate the integral:

$$(B.1) \quad z(t) = \int_{-\infty}^t \alpha(t-s) \odot r(s) ds \approx \int_{t-\Delta t_h}^t \alpha(t-s) \odot r(s) ds.$$

The memory horizon, $\Delta t_h \in \mathbb{R}_{>0}$, can, e.g., be determined with the bisection approach described in Section 6.1.

B.1. Non-stiff systems. For non-stiff systems, we obtain the approximate system

$$(B.2a) \quad x_{n+1} = x_n + f(x_n, z_n)\Delta t,$$

$$(B.2b) \quad z_{n+1} = \sum_{j=1}^{N_h} \alpha(j\Delta t) \odot r_{n-j+1}\Delta t,$$

$$(B.2c) \quad r_{n+1} = h(x_{n+1}),$$

where $t_n = t_0 + n\Delta t \in \mathbb{R}$ for some time step size, $\Delta t \in \mathbb{R}_{>0}$. We assume that the memory horizon is a multiple, $N_h \in \mathbb{N}$, of the time step size, Δt . For $t_n \leq t_0$, $x_n \in \mathbb{R}^{n_x}$ and $z_n, r_n \in \mathbb{R}^{n_z}$ are equal to $x(t_n)$, $z(t_n)$, and $r(t_n)$, and for $t_n > t_0$, they are approximations. This is an *explicit* approach, i.e., for given values of x_n , z_n , and r_n , z_{n+1} can be computed using (B.2b) and x_{n+1} can be evaluated with (B.2a). Finally, r_{n+1} can be evaluated with (B.2c), and the process is repeated for the subsequent time steps.

B.2. Stiff systems. For stiff systems, the approximate system is

$$(B.3a) \quad x_{n+1} = x_n + f(x_{n+1}, z_{n+1})\Delta t,$$

$$(B.3b) \quad z_{n+1} = \sum_{j=0}^{N_h-1} \alpha(j\Delta t) \odot r_{n-j+1}\Delta t,$$

$$(B.3c) \quad r_{n+1} = h(x_{n+1}),$$

which is a set of algebraic equations that, in general, must be solved numerically. In this work, we solve the residual equation

$$(B.4) \quad R_n(x_{n+1}; x_n) = x_{n+1} - x_n - f(x_{n+1}, z_{n+1})\Delta t = 0,$$

for each time step sequentially. Here, $R_n : \mathbb{R}^{n_x} \times \mathbb{R}^{n_x} \rightarrow \mathbb{R}^{n_x}$ is a residual function, and we consider z_{n+1} and r_{n+1} to be functions of x_{n+1} . Many numerical methods for solving nonlinear equations can utilize the Jacobian of the involved residual function. The Jacobian of the residual function in (B.4) is given by

$$(B.5) \quad \frac{\partial R_n}{\partial x_{n+1}}(x_{n+1}; x_n) = I - \left(\frac{\partial f}{\partial x}(x_{n+1}, z_{n+1}) + \frac{\partial f}{\partial z}(x_{n+1}, z_{n+1}) \frac{\partial z_{n+1}}{\partial x_{n+1}} \right) \Delta t,$$

where $I \in \mathbb{R}^{n_x \times n_x}$ is an identity matrix and the Jacobians of the memory state and the delayed variables are

$$(B.6a) \quad \frac{\partial z_{n+1}}{\partial x_{n+1}} = (\alpha(0)e^T) \odot \frac{\partial r_{n+1}}{\partial x_{n+1}} \Delta t,$$

$$(B.6b) \quad \frac{\partial r_{n+1}}{\partial x_{n+1}} = \frac{\partial h}{\partial x}(x_{n+1}).$$

Here, $e \in \mathbb{R}^{n_z}$ is a column vector of ones.

Appendix C. Kernels in the molten salt reactor model. In this appendix, we describe the kernel in the molten salt nuclear reactor model from Section 8.2. The i 'th kernel, $\alpha_i : \mathbb{R} \rightarrow \mathbb{R}_{\geq 0}$, is given by

$$(C.1) \quad \alpha_i(t) = \gamma_i e^{-\lambda_i t} \sum_{j=1}^{N_s} F(t; \mu_j, \sigma_j), \quad i = 1, \dots, N_g,$$

where $\gamma_i \in \mathbb{R}_{>0}$ is a normalization constant, $F : \mathbb{R}_{\geq 0} \times \mathbb{R} \times \mathbb{R}_{>0} \rightarrow \mathbb{R}_{\geq 0}$ is the folded normal kernel (8.2), and $N_s = 7 \in \mathbb{N}$ is the number of terms. The sum of folded normal kernels represents a nonuniform velocity profile in the external circulation of the molten salt (and neutron precursors), and the second factor describes the decay of the neutron precursors during the external circulation. For given $\mu_1 \in \mathbb{R}$ and $\sigma_1 \in \mathbb{R}_{>0}$, the location and scale parameters are

$$(C.2) \quad \sigma_{j+1} = \frac{3}{2}\sigma_j, \quad \mu_{j+1} = \mu_j + \sigma_j, \quad j = 1, \dots, N_s - 1.$$

Finally, the normalization constant is

$$(C.3) \quad \gamma_i = \left(\sum_{j=1}^{N_s} \frac{1}{2} e^{\frac{1}{2}\sigma_j^2 \lambda_i^2} \left(e^{\lambda_i \mu_j} \left(1 - \operatorname{erf} \left(\frac{\lambda_i \sigma_j^2 + \mu_j}{\sqrt{2}\sigma} \right) \right) + e^{-\lambda_i \mu_j} \left(1 - \operatorname{erf} \left(\frac{\lambda_i \sigma_j^2 - \mu_j}{\sqrt{2}\sigma} \right) \right) \right) \right)^{-1},$$

for $i = 1, \dots, N_g$.